Research Repository UCD

Title	Tyr728 in the Kinase Domain of the Murine Kinase Suppressor of RAS 1 Regulates Binding and Activation of the Mitogen-activated Protein Kinase Kinase
Authors(s)	Sibilski, C., Mueller, T., Kollipara, L., et al.
Publication date	2013-10-24
Publication information	Sibilski, C., T. Mueller, L. Kollipara, and et al. “Tyr728 in the Kinase Domain of the Murine Kinase Suppressor of RAS 1 Regulates Binding and Activation of the Mitogen-Activated Protein Kinase Kinase” 288, no. 49 (October 24, 2013).
Publisher	American Society for Biochemistry and Molecular Biology
Item record/more information	http://hdl.handle.net/10197/5571
Publisher's statement	This research was originally published in Journal of Biological Chemistry. C. Sibilski, T. Mueller, L. Kollipara, R. P. Zahedi, U. R. Rapp, T. Rudel, & A. Baljuls. "Tyr728 in the Kinase Domain of the Murine Kinase Suppressor of RAS 1 Regulates Binding and Activation of the Mitogen-activated Protein Kinase Kinase" . Journal of Biological Chemistry 2013 288: 35237-35252. © the American Society for Biochemistry and Molecular Biology.
Publisher's version (DOI)	10.1074/jbc.M113.490235

Downloaded 2023-10-05T14:16:07Z

The UCD community has made this article openly available. Please share how this access benefits you. Your story matters! (@ucd_oa)

© Some rights reserved. For more information

Tyr728 in the Kinase Domain of the Murine Kinase Suppressor of RAS 1 regulates Binding and Activation of the Mitogen-activated Protein Kinase Kinase*

Claudia Sibilski[‡], Thomas Mueller[§], Laxmikanth Kollipara[#], René P. Zahedi[#], Ulf R. Rapp[‡¶], Thomas Rudel[‡1], and Angela Baljuls[‡‖2]

From the [‡]Department of Microbiology, Biocenter, University of Wuerzburg, Germany; [§]Department of Molecular Plant Physiology and Biophysics, Julius-von-Sachs Institute for Biosciences, University of Wuerzburg, Germany; [#]Leibniz-Institut für Analytische Wissenschaften – ISAS – e.V., Dortmund, Germany; [¶]Division Molecular Mechanisms in Lung Cancer, Max Planck Institute for Heart and Lung Research, Bad Nauheim, Germany; [‖]Systems Biology Ireland, Conway Institute, University College Dublin, Ireland

*Running title: *Tyr728 is a Novel Regulatory Phosphorylation Site of Mouse KSR1*

[1]To whom correspondence should be addressed: Department of Microbiology, Biocenter, University of Wuerzburg, Am Hubland, 97074 Wuerzburg, Germany. Tel.: 49-931-31-84401; Fax: 49-931-31-84402; E-mail: thomas.rudel@biozentrum.uni-wuerzburg.de.
[2]To whom correspondence should be addressed: Systems Biology Ireland, Conway Institute, University College Dublin, Belfield, Dublin 4, Ireland. Tel.: 353-1-7166979; E-mail: angela.baljuls@ucd.ie.

Keywords: MAPK signal transduction; KSR1; RAF; tyrosine phosphorylation; LCK

Background: KSR1 coordinates the assembly of RAF/MEK/ERK complexes and regulates signal transduction.
Results: LCK-dependent phosphorylation of KSR1 on Tyr728 regulates MEK binding and activation.
Conclusion: Tyr728 phosphorylation may coordinate the transition between the scaffolding and catalytic function of KSR1 to fine-tune cellular responses.
Significance: Tyrosine phosphorylation of KSR1 is a new regulatory link between Src family kinases and RAF/MEK/ERK signaling.

ABSTRACT

In metazoans, the highly conserved MAPK signaling pathway regulates cell fate decision. Aberrant activation of this pathway has been implicated in multiple human cancers and some developmental disorders. KSR1 functions as an essential scaffold that binds the individual components of the cascade and coordinates their assembly into multiprotein signaling platforms. The mechanism of KSR1 regulation is highly complex and not completely understood. In this study we identified Tyr728 as a novel regulatory phosphorylation site in KSR1. We show that Tyr728 is phosphorylated by LCK, uncovering an additional and unexpected link between Src kinases and MAPK signaling. To understand how phosphorylation of Tyr728 may regulate the role of KSR1 in signal transduction, we integrated structural modeling and biochemical studies. We demonstrate that Tyr728 is involved in maintaining the conformation of the KSR1 kinase domain required for binding to MEK. It also affects phosphorylation and activation of MEK by RAF kinases and consequently influences cell proliferation. Moreover, our studies suggest that phosphorylation of Tyr728 may affect the intrinsic kinase activity of KSR1. Together, we propose that phosphorylation of Tyr728 may regulate the transition between the scaffolding and the catalytic function of KSR1 serving as a control point used to fine-tune cellular responses.

The kinase suppressor of RAS (KSR) is an essential scaffold protein, which coordinates the assembly and localization of the RAF/MEK/ERK complexes and regulates fidelity, intensity and duration of MAPK signaling (for review see (1, 2)). Although KSR knockout mice are developmentally normal, they are less susceptible to RAS-mediated skin cancer (3), which

underscores the importance of KSR in the regulation of MAPK-mediated cell proliferation and tumorigenesis. In mammals, the KSR protein family consists of two members, KSR1 and KSR2. The KSR homologs expressed in *Drosophila* and *C. elegans*, and the mammalian KSR proteins share five highly conserved regions (CA1–5) (4–7). KSR family members are structurally related to RAF kinases. The CA3 domain is similar to the CRD (cysteine-rich domain) of RAF and is required for membrane recruitment of KSR. CA4 is a serine/threonine-rich region similar to CR2 (conserved region 2) of RAF, while CA5 is highly homologous to the kinase domain (CR3) of RAF proteins (1). Though KSR members contain a kinase domain, the issue, whether mammalian KSR has kinase activity or is a pseudokinase, is controversially discussed (8–13). The main argument for mammalian KSR being a pseudokinase is the substitution of a lysine residue in subdomain II of the KSR kinase domain, which is highly conserved in RAF and other kinases, and is considered essential for catalytic activity due to a coordination function in ATP binding (4, 5, 14). Interestingly, *C. elegans* KSR1 and *Drosophila* KSR contain the invariant lysine in subdomain II, which would suggest that they are catalytically competent (2). However, mutation of the invariant lysine residue in *Drosophila* KSR does not compromise its function suggesting that either KSR proteins do not require catalytic activity to maintain their functionality or the catalytic competence of KSR (in contrast to other kinases) does not absolutely require a lysine residue in this position (15).

KSR has been shown to associate with RAF, MEK and ERK and to promote the formation of large molecular weight complexes for facilitating signal transduction (10, 16). MEK is constitutively associated with KSR, while RAF and ERK bind only in response to a stimulus (1, 17). ERK binds to the CA4 of KSR that includes a FXFP motif. This motif is also known as the DEF (docking site for ERK) domain (18, 19). The interaction with MEK is mediated by the CA5 of KSR. The recently published structure of the kinase domain of KSR2 in complex with MEK1 revealed that interaction between KSR and MEK occurs in a face-to-face manner involving their respective activation segments and αG helices, while association of KSR with RAF utilizes the side-to-side dimerization interface (13, 20).

Regulation of the KSR scaffolding property is complex and, to date, not fully understood. Numerous factors, including binding to 14-3-3, heat shock proteins 70 and 90, cdc37 and G-protein γ subunit, phosphorylation by PKA, C-TAK1 and ERK, and dephosphorylation by PP2A have been reported to regulate KSR functions (10, 17, 21–25). The binding of heat shock proteins and cdc37 to KSR is required for protein stability, as pharmacologically induced disruption of these interactions results in rapid KSR degradation (10). 14-3-3 binding regulates the recruitment of KSR to the plasma membrane and stabilizes the inactive and active conformations of KSR (17, 21). The recruitment of KSR to membrane compartments is a dynamic process that depends on C-TAK1-mediated phosphorylation and PP2A-dependent dephosphorylation of 14-3-3 binding sites located on either side of the CA3 domain in KSR (24, 25). The feedback phosphorylation by ERK promotes KSR1/B-RAF dissociation and the release of KSR1 from the plasma membrane (17, 26, 27).

Tyrosine kinases of the Src protein family are important regulators of the MAPK signal transduction pathway. It has been shown that Src activity is required for rapid activation of ERK signaling (28), and that Src kinases can phosphorylate several proteins of the cascade including EGFR, RAS-GAP and RAF (29–34). However, studies of mouse cells lacking three members of the Src family (Src, Yes, and Fyn) indicate that Src kinases are mostly dispensable for receptor tyrosine kinase signaling (35). Thus, the interplay between Src kinases and MAPK signaling is complex. In an effort to identify a new regulatory link between Src kinases and MAPK signal transduction we have searched for potential tyrosine phosphorylation site(s) in KSR1. Mass spectrometry analysis of mouse KSR1 coexpressed with LCK (the lymphocyte-specific member of the Src family) identified Tyr728 as a novel phosphorylation site. The LCK-mediated phosphorylation of Tyr728 was confirmed by substitution with non-phosphorylatable phenylalanine. To determine the role of Tyr728 phosphorylation in the regulation of KSR1 *in vivo*, we investigated the effect of Tyr728 substitution on KSR1/MEK interaction, MEK activation and cell proliferation. The *in vivo* studies were accomplished by *in silico* analysis of a KSR1 homology model structure and molecular dynamics simulations thereof. Here, we show that

the amino acid at position 728 has a dual importance for the functional properties of KSR1. First, it is involved in maintaining the 'bound' conformation of KSR1 kinase domain in complex with MEK and, therefore, influences KSR1/MEK association. Secondly, it affects phosphorylation of MEK by RAF and consequently influences cell proliferation. Moreover, our *in silico* studies suggest that phosphorylation of Tyr728 may affect the intrinsic kinase activity of KSR1. In conclusion, phosphorylation of Tyr728 may regulate the transition between the scaffolding and the catalytic function of KSR1 serving as a control point used to fine-tune cellular responses.

EXPERIMENTAL PROCEDURES

Cell lines, plasmids and antibodies—Immortalized KSR1$^{-/-}$ mouse embryonic fibroblasts (MEFs) and retroviral vectors (empty and KSR1-carrying MSCV-IRES-GFP as well as an ecotropic packaging vector) were kindly provided by the group of Robert E. Lewis (University of Nebraska Medical Center, Omaha). Anti-LCK (sc-433), anti-MEK1 (sc-219), anti-B-RAF (sc-166), anti-GFP (sc-9996), and anti-Actin (sc-1616) antibodies were obtained from Santa Cruz Biotechnology. Anti-phospho-MEK1/2 (9121) antibody was from Cell Signaling Technology. Anti-GST (A5800) antibody was purchased from Invitrogen. Anti-KSR1 (611576) was from BD Biosciences. Anti-phospho-Tyr (clone 4G10) antibody was produced in house.

Cloning of GST-tagged KSR1 wild type and mutants—Murine KSR1 cDNA was amplified by PCR. The upstream primer sequence was 5'-GGACTAGTATGGATAGAGCGGCGTTGCG-3', which contained a SpeI restriction site (underlined). The downstream primer sequence with a NotI restriction site (underlined) was 5'-ATTTGCGGCCGCCTAATGGTGATGGTGATG GTG-3'. KSR1 cDNA and the mammalian expression vector pEBG were cut with SpeI and NotI enzymes and, subsequently, ligated by use of T4 DNA ligase to give the expression plasmid for N-terminal GST-tagged and C-terminal his-tagged murine KSR1. The *Pfu* DNA polymerase was purchased from Agilent Technologies. Restriction enzymes and T4 DNA ligase were obtained from Thermo Scientific.

The site-specific mutations in the kinase domain of KSR1 were introduced using QuikChange site-directed mutagenesis kit (Agilent Technologies) according to the manufacturer's instructions. Mutations were verified by DNA sequencing.

Cell culture and transfection—COS7 and 293T cells were grown in DMEM (Sigma) containing 10% FBS (PAA Laboratories) and 2% penicillin/streptomycin (Gibco). KSR1$^{-/-}$ MEFs were cultivated in DMEM supplemented with 10% FBS, 1% penicillin/streptomycin and 0.1mM minimum essential medium with non-essential amino acids (MEM with NEAA, Gibco).

COS7 cells were transiently transfected with a total of 8µg of recombinant DNA per 10cm-dish using jetPEI transfection reagent (Polysciences, Inc.) according to the manufacturer's instructions.

Generating of stable cell lines—KSR1 retroviruses were generated by cotransfecting KSR1-carrying MSCV-IRES-GFP retroviral expression plasmids with an ecotropic packaging vector into 293T cells. Viral supernatants were then used to infect KSR1$^{-/-}$ MEFs in the presence of 6µg/ml polybrene. Control cells were infected with retroviruses carrying empty vector (MSCV-IRES-GFP). Pools of GFP-expressing MEFs were sorted by FACS according to increasing levels of fluorescence. For measuring the baseline fluorescence uninfected cells were used. Expression of KSR1 was proportional to the GFP expression level. KSR1 and GFP expression was confirmed by SDS-PAGE and Western blot analysis.

Proliferation assay—To synchronize the cell cycle, MEFs were starved for 24h in medium containing 0.5% FBS. After synchronization, MEFs were seeded in triplicate 6-well plates (3×10^4 cells/well) and cultivated in medium containing 10% FBS for 3 days. To keep the cells in the exponential growth phase over the timeframe of the assay, MEFs were trypsinized, counted by FACS, and seeded again (2×10^4 cells/well). The procedure was repeated three more times and the assay was stopped on day 12 after the first seeding.

Coprecipitation assay—24h post-transfection, cells were lysed with CoP buffer containing 10mM Tris-HCl (pH 8.0), 50mM sodium chloride, 30mM sodium pyrophosphate, 1mM sodium orthovanadate, 1% (v/v) Nonidet P-40 (NP-40), and a mixture of protease inhibitors (Roche) for 1h with gentle rotation at 4°C. All lysates were clarified by centrifugation at 16,100×g for 15min at 4°C. GST-tagged KSR1 was precipitated by incubating the supernatants with 80µl of

glutathione-sepharose beads (GE Healthcare) for 3-4h at 4°C with rotation. After incubation, the beads were washed three times with CoP buffer containing 0.1% (v/v) NP-40, supplemented with Laemmli buffer and boiled for 5min at 100°C.

Isolation of GST-fused KSR1 for mass spectrometry (MS) analysis—For preparation of recombinant KSR1 protein, COS7 cells were seeded in 25 10cm-dishes and transfected with 6µg KSR1 and 2µg kinase-active LCK-Y505F. 24h post-transfection, cells were washed once with PBS followed by lysis with buffer containing 25mM Tris-HCl (pH 7.6), 150mM sodium chloride, 25mM β-glycerophosphate, 25mM sodium fluoride, 10mM sodium pyrophosphate, 10mM β-mercaptoethanol, 1mM sodium orthovanadate, 10% (v/v) glycerol, 0.75% (v/v) NP-40, and standard proteinase inhibitors for 1h with gentle rotation at 4°C. The lysates were clarified by centrifugation at 16,100×g for 15min at 4°C. The supernatant containing GST-tagged KSR1 protein was incubated with 1ml of glutathione-sepharose beads for 2h at 4°C with rotation. After incubation the beads were washed three times with buffer containing 25mM Tris-HCl (pH 7.6), 300mM sodium chloride, 25mM β-glycerophosphate, 25mM sodium fluoride, 10mM sodium pyrophosphate, 10mM β-mercaptoethanol, 1mM sodium orthovanadate, 10% (v/v) glycerol, 0.2% (v/v) NP-40, and standard proteinase inhibitors. Beads were poured into a column and GST-KSR1 was eluted with 3ml buffer containing 50mM Tris-HCl (pH 8.0), 20mM glutathione, 1mM sodium orthovanadate, and standard proteinase inhibitors by collecting several fractions. The purity of recombinant KSR1 was documented by SDS-PAGE, Western blot analysis and staining with Coomassie Blue.

In gel-digestion for MS analysis—Approximately 2µg of each sample were separated by SDS-PAGE, proteins were then visualized by silver staining and digestion of excised gel slices was done as described previously (36).

In-solution digestion for MS—In-solution digestion was performed according to Burkhart *et al.* (37). Briefly, an aliquot of each sample corresponding to ~20µg of protein was diluted to 200µl with 50mM ammonium bicarbonate. Disulfide bonds were reduced using 10mM DTT for 30min at 56°C and free thiols were subsequently alkylated with 30mM iodoacetamide for 30min at room temperature in the dark. Trypsin (Promega) was added in a 1:25 (w/w) enzyme to substrate ratio and samples were incubated overnight at 37°C. Alternatively, samples were digested with 1:20 (w/w) Pronase E (*S. griseus*, Sigma-Aldrich) for 1h at 40°C, in the presence of phosSTOP (Roche Diagnostics). Digestion efficiency was monitored as described previously (37).

Enrichment of phosphopeptides—Peptides generated from both enzymatic digestions were acidified with 2% TFA and desalted using C18 solid phase extraction tips (OMIX, Agilent Technologies) according to the manufacturer's instructions. Subsequently, titanium dioxide-based phosphopeptide enrichment was conducted as described previously (38). All obtained eluates were analyzed using LC-MS/MS.

LC-MS/MS analysis—Samples were analyzed on LTQ-Orbitrap XL or LTQ-Orbitrap Velos mass spectrometers (Thermo Scientific), both online coupled to Ultimate 3000 RSLC systems (Thermo Scientific). Peptides were loaded in 0.1% TFA on a C18 trapping column (Acclaim Pepmap RSLC, 100µm×2cm, Thermo Scientific) and separated on a C18 main column (Acclaim Pepmap RSLC, 75µm×15cm) using a binary gradient (A: 0.1% formic acid; B: 0.1% formic acid, 84% acetonitrile) ranging from 5-50% B in 49min, at a flow rate of 300nl/min. Dedicated wash blanks were introduced between consecutive samples to eliminate memory effects (39). MS survey scans were acquired in the Orbitrap from m/z 300 to 2000 at a resolution of 60,000 using the polysiloxane m/z 445.120030 as lock mass (40). The five most intense signals were subjected to collision-induced dissociation (CID) in the ion trap, using multistage activation (MSA) and taking into account a dynamic exclusion of 30s. CID spectra were acquired with a normalized CE of 35%, an isolation width of 2m/z, an activation time of 30ms and a maximum injection time of 100ms. For MSA, neutral losses of phosphoric acid and water were considered. Automatic gain control target values were set to 10^6 for MS and 10^4 for MS/MS scans.

MS data processing and interpretation—Raw MS data were converted into mgf format using the ProteoWizard software 2.2.0 (41). Obtained peak lists were searched against a concatenated target/decoy version of the UniProt mouse database, including isoforms, using Mascot 2.4 (Matrix Science), OMSSA 2.1.9 and X!Tandem (version 01.01.2010) with the help of searchGUI 1.10.4 (42). Trypsin with a maximum of two

missed cleavages was selected as enzyme, whereas no enzyme was chosen for Pronase E samples. Phosphorylation of Ser/Thr/Tyr was selected as variable modification. MS and MS/MS tolerances were set to 10ppm and 0.4Da, respectively. Finally, validation of identified peptides and phosphopeptides was done using the PeptideShaker software 0.18.3 (http://code.google.com/p/peptide-shaker/), applying a false discovery rate of 1% at the peptide-spectrum-match level. Only phosphorylation site localizations meeting the following criteria were considered as confident: (i) if the number of phosphorylations equals the number of potential phosphorylation sites, (ii) if the peptide is singly phosphorylated and passed a 1% false localization rate threshold, or (iii) if the peptide is multiply phosphorylated and has a D-score >95% (43).

Modeling of the three-dimensional structure of the mouse KSR1 kinase domain—The model of the mouse KSR1 kinase domain (UniProt identifier Q61097, residues Ser550 to Leu830) was built on the basis of the template structure of human KSR2 in complex with MEK1 (PDB entry 2Y4I, (13)). Sequence alignment between the target KSR1 and the template yielded an amino acid sequence identity of 69% and a homology of almost 86% over 280 residues. For modeling the KSR2 chain was stripped from the MEK1 molecule present in the structure of the complex and differing amino acid residues were exchanged to those present in mouse KSR1 using the ProteinDesign tool in the software package Quanta2008 (MSI Accelrys, San Diego). Two substitutions involved an exchange from another amino acid to a proline residue or vice versa. For all amino acid replacements rotamer searches were performed to minimize steric constraints before fitting in the side chain. A short energy minimization (50 steps of conjugate gradient minimization, all-hydrogen force field Charmm27, MSI Accelrys) using only geometrical energy terms with the backbone restrained with strong harmonic potential (energy constant 50kcal mol^{-1} $Å^{-2}$) was performed to allow bonds and angles of substituted residues to be relaxed. Finally, all exchanges could be performed without causing bad van der Waals contacts in the final structure of mouse KSR1. The interaction of KSR2 with MEK1 occurs mainly by facing their catalytic sites, implicating activation segment and αG helix, respectively, each other (13).

Molecular dynamics (MD) simulations of KSR1 kinase domain—To test the influence of the phosphorylation onto the structure of KSR1 kinase domain, MD simulations in explicit water were performed using the software package NAMD/VMD (version 2.9). The model structures of the Tyr728-phosphorylated and non-phosphorylated mouse KSR1 variants were first energy minimized in Quanta2008 (MSI Accelrys) to remove possible bad van der Waals contacts using only geometrical energy terms employing 500 steps conjugate gradient minimization and the Charmm27 all-hydrogen force field. Then the model structures were placed into a rectangular water box (TIP3 water) to cover the protein with an at least 25Å thick solvent layer yielding a final box with dimensions 93×92×100Å. The overall charge of the box containing protein and solvent was then first neutralized by the module autoionize 1.3 and then to add additional 150mM potassium chloride. For the KSR1 model with phospho-Tyr728 the box contained besides the protein molecule (residues Ser550 to Leu830) 25,344 TIP3 water molecules, 72 chloride ions, 76 potassium ions, one magnesium ion, and one ATP molecule. For the KSR1 model with non-phosphorylated Tyr728 the same procedure was applied. For simulations, the Charmm27 all-hydrogen force field was used, periodic boundaries were set to the above described box dimensions and Particle Mesh Ewald method was applied to the box to treat electrostatic interactions. A cutoff of 12Å was chosen for van der Waals and electrostatic interactions with a switching function starting at a distance of 10Å. All simulations were performed as Langevin dynamics at a temperature of 310K, a damping coefficient of $1ps^{-1}$ and constant pressure of 1.01325bar with a time step of 1 (or 2 for final minimization and production) fs. Bonds involving hydrogens were kept rigid by applying the SHAKE algorithm. The system KSR1-phospho-Tyr728 containing 80,780 atoms in total (KSR1-Tyr728: 80,773 atoms) was then equilibrated in a stepwise procedure. First a 0.5ns trajectory with all protein heavy atoms including the ATP molecule and the magnesium ion kept fixed was performed to allow for minimization of the hydrogens, the solvent molecules as well as the ions to allow for proper distribution of the ions within the box. Then protein and ATP atoms were stepwise released, first with a short 0.1ns trajectory and a harmonic potential on

protein/ATP heavy atoms of 20kcal mol^{-1} $Å^{-2}$, then another 0.1ns simulation by employing 4kcal mol^{-1} $Å^{-2}$ harmonic restraints and then a final 0.5ns minimization with no restraints. Then a production trajectory was calculated with 5ns duration (2fs time steps). The final 5ns trajectories were analyzed in VMD with respect to hydrogen bond formation and root mean square (r.m.s.) deviation of various secondary structure and loop elements.

RESULTS

LCK interacts with KSR1 for tyrosine phosphorylation—In its amino acid sequence and the pattern of regulation, KSR1 shows a high homology to RAF kinases, which are known to be regulated by Src family kinases (32, 33). Therefore, we hypothesized that KSR1 may also be phosphorylated and regulated by tyrosine kinases of the Src protein family. To test this assumption we coexpressed GST-fused murine KSR1 with active (Y505F) or inactive (K273E/Y505F) LCK mutants in COS7 cells and precipitated KSR1 with glutathione-sepharose beads. As shown in Fig. 1*A*, KSR1 coexpressed with the active LCK was tyrosine phosphorylated. In contrast, no tyrosine phosphorylation was found in the KSR1 sample coexpressed with kinase-inactive LCK, suggesting that LCK binds and phosphorylates KSR1 on as yet unknown tyrosine residue(s). These results were confirmed by use of LCK inhibitor III (Calbiochem, 428207). Treatment of cells with the inhibitor completely abolished the LCK-induced tyrosine phosphorylation of KSR1 (Fig. 1*B*).

MS analysis of KSR1 identified Tyr728 as a target for LCK-mediated phosphorylation—We next searched for candidate tyrosine residues in KSR1 that can be phosphorylated by Src family kinases. *PhosphoSitePlus* (a database of observed post-translational protein modifications) refers Tyr673 of mouse KSR1 as a potential phosphorylation site identified by MS analysis (www.phosphosite.org). To prove whether Tyr673 is a target for LCK-mediated phosphorylation and to identify further candidate tyrosine residue(s), which might be phosphorylated by LCK, we performed MS analysis of GST-KSR1 coexpressed with active LCK-Y505F mutant in COS7 cells and purified by binding to glutathione-sepharose. Three independent MS measurements provided up to 78% coverage of the entire protein sequence. The combined results obtained for murine KSR1 phosphorylation are summarized in Fig. 2*A*. Besides several serine and threonine residues known for phosphorylation in KSR1, we could identify 17 so far unknown confident phosphorylation sites. Intriguingly, one of the newly identified phosphorylation sites was Tyr728, which was detected only in the KSR1 sample coexpressed with LCK, suggesting that this tyrosine is phosphorylated by LCK. However, our MS analysis did not confirm phosphorylation of Tyr673.

Next, we mutated Tyr673 and Tyr728 to phenylalanine, a non-phosphorylatable amino acid, and tested whether any of the mutations would affect KSR1 phosphorylation by LCK. We found that the Y728F substitution greatly diminished, whereas Y673F increased KSR1 phosphorylation (Fig. 2*B* and *C*). Along with the MS data of the present study, these results suggest that Tyr728, but not Tyr673, is the major target for LCK-mediated phosphorylation of KSR1.

Tyr673 is important for the functional conformation of the KSR1 kinase domain—Tyr673 and Tyr728 are located within the kinase domain of KSR1 (Fig. 3*A* and *B*), which has been shown to bind and prime MEK1 for activating phosphorylation by RAF kinases (13). Remarkably, whereas Tyr673 is highly conserved between all KSR and RAF proteins, respectively, Tyr728 is conserved only between KSR1 proteins of different species and is replaced by histidine in KSR2 (Fig. 3*A* and *B*). Previously, the Tyr673 homologue in *Drosophila* RAF (Tyr538 in D-RAF) was also considered as a potential phosphorylation site, but was not confirmed experimentally. It was suggested that as a highly conserved amino acid, Tyr538 might be important for the functional structure of the D-RAF kinase domain. Indeed, it was shown that the Y538F mutation completely abolished the kinase activity of D-RAF (44). In light of these data we assumed that Tyr673 might be important for the structure of the KSR1 kinase domain, rather than being a regulatory phosphorylation site. To prove this assumption we tested, whether Tyr673 modification is important for the binding of MEK and B-RAF to KSR1 and for activating phosphorylation of MEK by RAF. We found that Y673F substitution impaired both, the binding of MEK and B-RAF to KSR1 (Fig. 3*C*, *E* and *F*). Moreover, phosphorylation of the KSR1-Y673F-bound MEK was strongly diminished compared to

KSR1 WT-bound MEK, resulting in a reduced phospho-MEK level in lysates (Fig. 3*C* and *D*). These results support the assumption that similar to Tyr538 of D-RAF, Tyr673 is important for maintaining the functional conformation of the KSR1 kinase domain.

Tyr728 regulates the activating phosphorylation of MEK—We next explored whether Tyr728 is important for MEK activation. To this end we tested the binding of MEK and B-RAF to KSR1-Y728F mutant and phosphorylation of KSR1-Y728F-bound MEK in a coprecipitation assay. The results of these experiments revealed that although the binding of MEK to KSR1 was dramatically reduced by Y728F substitution, the activating Ser218 and Ser222 phosphorylation of the KSR1-Y728F-bound MEK was three times higher than the phosphorylation of MEK bound to KSR1 WT (Fig. 4*A* and *B*). Furthermore, binding of B-RAF to KSR1-Y728F mutant was increased compared to WT (Fig. 4*C* and *D*). These results are consistent with the idea that Tyr728 of KSR1 plays a regulatory role in the mechanism of MEK activation and suggest that phosphorylation of Tyr728 may interfere with the activating phosphorylation of MEK by B-RAF.

Phosphorylation of Tyr728 negatively regulates cell proliferation—KSR is known as a general positive mediator of MAPK signaling. ERK stimulation in the absence of KSR was attenuated in a variety of systems, including tumor growth and T cell activation (16). Our experimental data suggest that phosphorylation of KSR1 on Tyr728 negatively regulates MEK activation by B-RAF and may result in inhibition of cellular processes depending on MAPK signal transduction. To test the effect of Tyr728 phosphorylation on cell proliferation we used MEFs derived from KSR1 deficient mice ($KSR1^{-/-}$ MEFs) (16, 45). $KSR1^{-/-}$ MEFs were infected with retroviruses for stable expression of KSR1 WT or KSR1-Y728F mutant. As shown in Fig. 5, proliferation of MEFs stably expressing KSR1 WT was almost unchanged compared to MEFs infected with empty vector. In contrast, MEFs expressing KSR1-Y728F proliferated significantly faster than MEFs infected with KSR1 WT. These results are consistent with the data showing that Y728F substitution increases activating phosphorylation of KSR1-bound MEK by B-RAF (Fig. 4), supporting the assumption that phosphorylation of Tyr728 in KSR1 may interfere with the B-RAF-mediated activation of MAPK signaling and as a consequence delay cell proliferation.

Conformational rearrangement of the KSR1 kinase domain is required for phosphorylation of Tyr728—To obtain insights into possible mechanisms by which Tyr728 phosphorylation may regulate the function of KSR1, we performed modeling of KSR1 kinase domain (KD) with and without Tyr728 phosphorylation. In addition, a homology model for the interaction of KSR1(KD) with MEK1 was built. For modeling we used the recent structure analysis of the protein-protein complex of human KSR2(KD) bound to rabbit MEK1 as a template (13). Due to the very high homology between the kinase domains of mouse KSR1 and human KSR2, comprising 69% sequence identity on the amino acid level (86% sequence homology), the KSR1(KD) model could be built without requiring manual loop building or modeling of deletions and thus provides a valid KSR1(KD) model for further structural and functional analyses. The modeling revealed that in the 'bound' conformation, as in KSR2(KD) in complex with MEK1, the Tyr728 of KSR1(KD), which is located in a short helical element just C-terminal of the activation segment and ahead of αEF helix, is buried inside the core of the kinase domain (Fig. 6*A* and *B* and Fig. S1*A* and *B*). This suggests that for phosphorylation of Tyr728 a conformational rearrangement compared to the 'bound' conformation of KSR2(KD) in complex with MEK1 (PDB entry 2Y4I) must occur. However, as the activation segment consists of a rather long loop with a large number of polar and/or charged residues and no stabilizing secondary structure, it seems very likely that in its unbound state (i.e. not interacting with MEK1) the activation segment is not conformationally restrained and thus Tyr728 might be placed at the protein surface accessible for phosphorylation by LCK. This interpretation is consistent with the observation that even in the complex of KSR2(KD) bound to MEK1 a part of the activation segment of KSR2(KD) has no observable electron density due to disorders (13). In contrast, Tyr673 is also partially buried in the kinase domain, but in comparison to Tyr728 it is a part of a conformationally restrained helical element (see Fig. 6*C*). Therefore, it is most likely that Tyr673 is not accessible to modification by tyrosine kinases, which is in accordance with our results obtained for substitution.

The model of KSR1 in Fig. 6*B* also shows that the phospho-moiety of phospho-Tyr728 forms a network of direct hydrogen bonds with several surrounding residues located in helical elements, such as αD helix (His645, Arg649) and αF helix (Glu763). Arg649 might serve as an anchor point for the phosphate group of phospho-Tyr728. When the KSR1(KD)-phospho-Tyr728 model was compared with a model containing a non-phosphorylated Tyr728 residue, no direct hydrogen bonds between the tyrosine hydroxyl group and surrounding residues could be found (Fig. S1*A* and *B*). This might hint towards an (locally) increased stability of the KSR1(KD) structure when Tyr728 is phosphorylated, which in turn might alter MEK and/or RAF binding. The model-derived prediction is consistent with the experimental data obtained for Y728F mutant, which showed strongly reduced MEK binding, but increased interaction with B-RAF (Fig. 4*A*, *C* and *D*).

Additionally, to test whether the interaction between KSR1(KD) and MEK differs significantly from the KSR2(KD)/MEK interaction shown in the published structure analysis (13), we have docked the model obtained for murine KSR1(KD) onto the template complex KSR2(KD)/MEK1 (PDB entry 2Y4I). The kinase-kinase interface is located in the lower lobes of both kinases and the contact between the αG helices of both kinase domains contributes the largest surface to this interaction (Fig. 6*C* and *D*). Interestingly, all residues in this helix, which are in direct contact with residues of MEK1, are invariant between KSR1 and KSR2 indicating that the interaction mechanism for this kinase-kinase interaction is likely to be highly similar.

Arg649 stabilizes the 'bound' conformation of KSR1 kinase domain in complex with MEK—Next, we tested, whether substitution of Arg649 (a predicted anchor point for the phosphate group of phospho-Tyr728) with alanine or glutamic acid might impair stability of the KSR1 kinase domain and thereby alter the KSR1/MEK interaction. The results of this experiment revealed that similar to KSR1-Y728F mutant, substitution of Arg649 either strongly reduced (R649A) or completely abolished (R649E) the KSR1/MEK association (Fig. 7*A*). These data support the model-derived assumption that Arg649 might be involved in stabilization of the 'bound' conformation of KSR1 kinase domain in complex with MEK. Consistent with this idea, we found that exchange of Arg649 resulted in increased binding of LCK to KSR1 leading to a remarkably higher Tyr728 phosphorylation level compared to KSR1 WT (Fig. 7*A*). This suggests that amino acid exchanges at position 649 might shift the equilibrium of KSR1 folding states toward the conformation, in which Tyr728 is placed at the protein surface accessible for phosphorylation by LCK.

Chemical structure of the amino acid at position 728 determines functional properties of KSR1—We have shown that the MEK-binding ability of KSR1 mutants Y728F and R649A is strongly reduced compared to WT (Figs. 4*A* and 7*A*). However, these substitution mutants behaved differently with respect to phosphorylation of KSR1-bound MEK. Whereas the phosphorylation of the KSR1-R649A-bound MEK was unchanged, the phosphorylation of MEK in the complex with KSR1-Y728F was three times higher than the phosphorylation of MEK bound to KSR1 WT (compare Fig. 7*A* with Fig. 4*A* and *B*). To test whether this effect is specific for tyrosine to phenylalanine exchange or is general for substitution with any amino acid at this position, we generated Y728A and Y728E substitutions in KSR1 and analyzed their competence for MEK binding and phosphorylation of KSR1-bound MEK. We found that similar to the substitution with phenylalanine, the MEK binding to Y728A mutant was significantly reduced, whereas the phosphorylation of KSR1-Y728A-bound MEK was markedly increased compared to WT. Substitution of Tyr728 with negatively charged glutamic acid completely abolished binding of MEK to KSR1 (Fig. 7*B* and *C*). Interestingly, in KSR2 the Tyr728 of KSR1 is replaced by histidine (His841, see also Fig. 3*B*). Therefore, we decided to test whether substitution of Tyr728 to histidine may have any effect on KSR1 functionality. Surprisingly, Y728H mutation did not change the association between KSR1 and MEK, but it significantly reduced the phosphorylation of KSR1-bound MEK (Fig. 7*B* and *C*). Taken together, our substitution analysis revealed that the amino acid at position 728 has a dual importance for the functional properties of KSR1. First, it is involved in maintaining the 'bound' conformation of KSR1 kinase domain in complex with MEK and, therefore, influences KSR1/MEK association. Secondly, it affects phosphorylation of MEK. Our results also suggest that these two functions are in reciprocal relation to each other. The chemical structure of the amino acid at position 728, that

favors the tight binding of MEK, reduces phosphorylation of the bound MEK and vice versa.

Phosphorylation of Tyr728 induces conformational rearrangements in the MEK interface and affects structural elements involved in catalytic activity of KSR1—To test whether and how phosphorylation of Tyr728 in KSR1 might alter structure, potential kinase activity or the interaction of KSR1 with MEK, we performed MD simulations in explicit water. The model of the KSR1(KD) with or without Tyr728 phosphorylated was placed in a water box with ions at a concentration of 150mM to neutralize protein charges and 5ns unrestrained trajectories were calculated after stepwise minimization. Using VMD hydrogen bonding and r.m.s. deviation, fluctuations were checked for various elements in the kinase domain (Fig. 8). As suggested from the static starting model, hydrogen bonding between the side chain of Tyr728 and surrounding residues was stronger in case of the phospho-Tyr728 throughout the 5ns trajectory, in both, the numbers of hydrogen bonds as well as the duration of hydrogen bonding. This suggests that the helical element containing phospho-Tyr728 as well as elements, which are in contact with phospho-Tyr728, are possibly stabilized. The r.m.s. deviation analysis of the helix, which carries Tyr728 at its C-terminal end, shows that in the case of phospho-Tyr728 the conformational and positional variations of the backbone atoms are significantly lower (r.m.s. deviation about 2Å) compared to KSR1 with the non-phosphorylated Tyr728 (r.m.s. deviation between 2 and 4Å, see Fig. 8*B*). Other regions, similarly, appear less flexible in the MD simulations of KSR1 with phospho-Tyr728. For example, the activation loop (residues Ser707 to His723), which in kinases usually controls the access of the substrate to the active site and is displaced by phosphorylation of serine and/or threonine residues present in this segment, exhibits lower fluctuations for the backbone atoms when Tyr728 is phosphorylated (Fig. 8*C*). This may indicate that phosphorylation of Tyr728 leads to stabilization of the activation segment, which in turn potentially influences KSR1 kinase activity and/or stabilizes complex formation with MEK. Consistent with a potential effect on kinase activity is the observation that in KSR1 with phosphorylated Tyr728, the Lys685, which is involved in phosphate transfer, interacts with the phosphate group of phospho-Tyr728 and thus exhibits a highly restrained side chain conformation throughout the 5ns trajectory, whereas for KSR1 with non-phosphorylated Tyr728 the lysine residue is far more flexible (Fig. 9*A* and *B*). Other elements appear to be not affected significantly according to the MD simulation results. For example, the short helical element comprising Thr643 to Arg649, of which the latter residue might serve as an anchor point for the phosphate group of phospho-Tyr728, does not show any differences with respect to r.m.s. deviations of its backbone atoms (Fig. 8*D*). Neither does the catalytic loop segment carrying the conserved Asp683 and Lys685 residues, which are involved in transfer of the γ-phosphate group of the ATP onto the substrate, show a more stable backbone conformation when Tyr728 is phosphorylated (Fig. 8*E*).

To gain insights on whether the Tyr728 phosphorylation exerts a long-range effect by modulating the stability of the interface either to MEK (αG helix consisting of residues Glu777 to Ser785) or the potential binding site to the regulatory RAF kinase (loop element ahead of αC helix, residues Gln613 to Glu617) we analyzed the fluctuations of the backbone atoms in the trajectories of both models, KSR1-Tyr728 and KSR1-phospho-Tyr728, however, no significant differences could be observed in the r.m.s. deviation (Fig. 8*F* and *G*). Although the phosphorylation of Tyr728 does not lead to stabilization of the KSR1/MEK1 interface, analysis of the distances between the Cα-atom of Tyr728 and Ala778, which is on the MEK facing side of the αG helix and one of the KSR1 residues contacting MEK1, shows that in KSR1 with phospho-Tyr728 the Cα-Cα distance is shorter throughout the MD simulation compared to KSR1 with non-phosphorylated Tyr728 (Fig. 9*C* and *D*). Thus, a conformational rearrangement most likely induced by the higher stability of the activation loop in KSR1-phospho-Tyr728 leads to a more compact KSR1/MEK1 interface.

DISCUSSION

In the present study we have investigated the mechanism of KSR1 regulation by both structural modeling and biochemical means. We have identified a novel tyrosine residue (Tyr728) within the KSR1 kinase domain, which is phosphorylated by the Src kinase family member LCK and is important for binding and phosphorylation of

MEK *in vivo*. Structure modeling revealed that in the 'bound' conformation of KSR1 in complex with MEK, the Tyr728 is packed inside the core of the kinase domain and is likely not accessible to phosphorylation. This means that conformational rearrangement of the KSR1 kinase domain is required for placing the Tyr728 at the protein surface and making it accessible to modification by a tyrosine kinase. This consideration was confirmed by our experimental data. Arg649, which is conserved in KSR1 and KSR2, is thought to stabilize the 'bound' conformation of KSR1 kinase domain, because the cationic side chain of Arg649 is an anchor point for the phosphate residue of phospho-Tyr728 and it also possibly interacts with Trp769 (Fig. 6*B*). The latter so called cation-π interaction between the cationic side chain of an aliphatic amino acid and the side chain of an aromatic residue can significantly contribute to the stabilization of the protein secondary structure (46). Therefore, replacement of Arg649 was expected to relax the protein structure around the Tyr728 and make it accessible for phosphorylation. Indeed, substitution of Arg649 to alanine or glutamic acid led to enhanced binding of LCK accompanied by increased phosphorylation of Tyr728 (Fig. 7*A*). Similar to the data obtained for Arg649, replacement of Tyr673 with phenylalanine resulted in increased phosphorylation of Tyr728 (Fig. 2*B*). Tyr673 is highly conserved not only in KSR but also in RAF proteins and is considered to be important for maintaining the functional conformation of the kinase domain (44). Therefore, it is most likely that substitution of Tyr673 leads to partial unfolding of the kinase domain placing Tyr728 at the protein surface accessible for phosphorylation by LCK.

Phosphorylation of buried residues is not unique to KSR1. A substantial number of phosphorylation sites (15%) are actually packed into the domain core of proteins and not exposed to the solvent (47). The systematic comparative and structural analysis of phosphorylatable buried residues revealed that their modifications could have three major structural/functional effects: (i) regulation of function by affecting functional sites directly or indirectly, (ii) spatial rearrangements (presumably by rigid body movements) of domains within a protein, and (iii) opening of the structure, leading to local flexibility (47). Frequently, phosphorylatable buried residues are found at or close to active sites and binding pockets of proteins. There are numerous examples demonstrating that their phosphorylation affects either directly or indirectly the integrity of the functional sites depending on whether they are part or in the vicinity of them, respectively (47). According to the model of KSR1(KD) shown in Fig. 6, Tyr728 is located close to the catalytic loop and activation segment. These functional elements are present in every known protein kinase. The invariant aspartic acid of the catalytic loop (Asp683 in KSR1, see Fig. 3*A* and *B*) is presumed to act as a catalytic base to free up the hydroxyl oxygen on the substrate for nucleophilic attack (Figs. 6*B* and 9*A*). The activation loop often contains a phosphorylation site that upon phosphorylation induces a conformational change on the loop that allows the substrate to bind to the kinase and also positions the invariant aspartate group of the catalytic loop for phosphate transfer reaction (48). The close proximity of Tyr728 to these functional elements suggests that phosphorylation of this residue may influence the potential catalytic competence of KSR1. Indeed, our MD simulations support this assumption. The backbone atoms of the activation loop exhibit lower fluctuations when Tyr728 is phosphorylated (Fig. 8*C*). Moreover, the amino group of the conserved Lys685 in the catalytic loop seems conformationally fixed between the phosphate group of phospho-Tyr728 and the γ-phosphate group of the ATP molecule, such that it can ideally facilitate phosphate transfer from the ATP to an acceptor hydroxyl group in a substrate (Fig. 9*A* and *B*). Substitution of arginine for the conserved ATP-coordinating lysine residue in mammalian KSR proteins and the capacity of kinase-impaired mutants of KSR to mediate MEK phosphorylation and MAPK signaling have implicated KSR as a pseudokinase (10, 15). However, the protein structure of KSR2(KD) in complex with MEK1 indicates that KSR has the potential for catalytic activity (13). Indeed, it has been reported that KSR2 is the major kinase responsible for MEK1 phosphorylation at non-B-RAF sites (13). KSR2 is also capable to phosphorylate MEK1 at B-RAF sites (Ser218 and Ser222), however, with extremely low efficiency (13). Other groups reported kinase activity for KSR1 (11, 12, 49). Thus, a growing body of evidence supports the view that KSR can indeed act as a protein kinase. Therefore, implication of Tyr728 phosphorylation in regulation of KSR1 catalytic activity seems very likely.

The published structure of the KSR2(KD)/MEK1 heterodimer revealed that these two molecules interact with their catalytic sites facing each other through their activation segments and αG helices (13). Therefore, changes in the conformation of the activation segment in the kinase domain of KSR are supposed to affect not only the catalytic competence of KSR, but also its ability to bind MEK. As mentioned before, our static model of the KSR1(KD) bound to MEK revealed that Tyr728 is located in a short helical element just C-terminal of the activation segment. The hydroxyl group of the non-phosphorylated Tyr728 forms a network of interactions with surrounding residues, which may stabilize the conformation of the activation segment required for the binding to MEK (supplemental Fig. S1*B*). Indeed, substitution of Tyr728 with phenylalanine or alanine – the neutral residues that do not form any stabilizing interactions with surrounding residues in our model – resulted in strongly reduced MEK binding to KSR1 (Figs. 4*A* and 7*B*). Phosphorylated Tyr728 may stabilize the functional conformation of the activation segment even more efficiently, since the network of interactions is extended by several direct hydrogen bonds between the phosphate group and the surrounding residues (compare supplemental Fig. S1*A* and *B*). According to our model phosphomimetic amino acid, such as glutamic acid, at position 728 would not substitute for phosphorylated Tyr and also not for non-phosphorylated Tyr in terms of stabilization of the activation segment, because its predicted pattern of interactions with surrounding residues differs substantially from that of Tyr and phospho-Tyr (compare supplemental Fig. S1*A*, *B* and *D*). Consistently, the replacement of Tyr728 with glutamic acid completely abolished binding of KSR1 to MEK (Fig. 7*B*). Moreover, our MD simulations revealed that the distance between the Cα-atom of Tyr728 and Ala778 residue of the αG helix is smaller, if Tyr728 is phosphorylated (Fig. 9*C* and *D*). Thus, a more compact interface might be formed, possibly facilitating MEK binding to KSR1. Together, our data strongly suggest that chemical properties of the amino acid at position 728 may define the flexibility of the activation segment over time and as a consequence affect the stability of the interaction between the KSR1 kinase domain and MEK.

KSR/MEK heterodimers assemble KSR/MEK heterotetramers or KSR/MEK/RAF ternary complexes via side-to-side dimerization of two KSR molecules or of KSR and RAF molecules, respectively. It has been suggested that in the KSR/MEK heterotetramer, the inaccessible activation segment of MEK is released through the interaction of KSR with a regulatory RAF molecule, allowing catalytic RAF to phosphorylate MEK (13). Our experimental data are in agreement with this hypothesis. We have shown that substitution of the tyrosine at the position 728 with phenylalanine, which is supposed to loosen the KSR1/MEK interaction, facilitated the KSR1/B-RAF heterodimerization and increased the activating phosphorylation of the KSR1-bound MEK (Fig. 4).

The MS analysis of the present study further identified Ser722 as a novel phosphorylation site of KSR1 (Fig. 2*A*). Phosphorylation of this residue was found in all replicates, suggesting that Ser722 is one of the major phosphorylation sites in mouse KSR1. Remarkably, Ser722 is located six residues ahead of Tyr728 in the linear sequence of amino acids and is part of the activation loop (Figs. 3*A* and 6*A*). Therefore, we propose that the phosphorylation of Ser722 may affect catalytic activity and/or substrate specificity of KSR1. Even more remarkable is the close proximity of Ser722 to the catalytic site in the model of KSR1(KD) (see Fig. 6*A* and *C*). Considering this fact, it is tempting to hypothesize that Ser722 might be an autophosphorylation site. Previous studies revealed that mammalian KSR1 is indeed capable of serine autophosphorylation, which likely occurs on a single or limited number of serine residues, since only a single migrating ^{32}P-labeled peptide was detected in 2D tryptic phosphopeptide mapping following *in vitro* kinase assay (49). Interestingly, Ser722 is conserved in KSR1 proteins of different species, but is replaced by a non-phosphorylatable amino acid (Gln835) in KSR2 (Fig. 3*A* and *B*). Consistently, no autophosphorylation of KSR2 has been reported so far. Taken together, the assemblage of facts supports the idea that Ser722 might be autophosphorylated in *cis*. In general, autophosphorylation of a critical residue in the activation loop is an essential maturation event required for full enzyme activity of several protein kinases (50–52). Therefore, the autophosphorylation of Ser722 may be crucial for the catalytic activity of KSR1. This assumption is supported by the observation that the substitution of the serine at the position 722 to alanine or

aspartic acid did not change the interaction between KSR1 and MEK, but strongly diminished the phosphorylation of KSR1-bound MEK (data not shown).

As pointed out before, there is no phosphorylation site in mammalian KSR2 at the position homologous to Ser722 of KSR1. Intriguingly, the KSR1-Tyr728 is also replaced by a non-phosphorylatable amino acid (His841) in KSR2 (Fig. 3*B*). The co-occurrence of these two substitutions in the course of KSR evolution supports the idea of a regulatory interrelation between the phosphorylation of Tyr728 and Ser722. In general, kinases that are autophosphorylated in *cis* are likely to have developed additional mechanisms to regulate their activity, including phosphorylation on other regions of the kinase (52). Phosphorylation of Tyr728 might be such an additional regulatory mechanism of the KSR1 kinase activity. Loss of the autophosphorylation site Ser722 in the activation segment would make the Tyr728-mediated regulation redundant. Therefore, mammalian KSR2, in which the autophosphorylation site in the activation segment was omitted, also lost the regulatory phosphorylation site at position homologous to Tyr728 of KSR1.

Previous study of the molecular mechanism, by which protein kinases phosphorylate their own activation loop, suggests that a canonical kinase domain can adopt a functional intermediate during maturation of the enzyme (52). As discussed before, the existence of such an intramolecular transitional intermediate is a *conditio sine qua non* for phosphorylation of KSR1-Tyr728 by LCK. Therefore, we hypothesize that LCK phosphorylates the nascent KSR1 kinase passing through a transitory intermediate. Our static model and molecular dynamics simulations suggest that in the mature kinase, phospho-Tyr728 locally stabilizes the functional element involved in catalytic reaction (Figs. 6, 8 and 9) and consequently may increase the likelihood of the activating Ser722 autophosphorylation resulting in enhanced catalytic activity of KSR1 towards MEK. In support of this hypothesis we found that the replacement of tyrosine at the position 728 with histidine, whose uncharged form is isosterically analog to tyrosine, did not change the interaction between KSR1 and MEK, but strongly decreased phosphorylation of the KSR1-bound MEK (Fig. 7*B* and *C*). This suggests that histidine at the position 728 can be tolerated with respect to KSR1/MEK interaction, but not with respect to catalytic activity of KSR1. These data are in line with the observation that KSR2, which binds MEK as efficient as KSR1, but has very low intrinsic kinase activity towards MEK (13), has a histidine at the position homologous to KSR1-Tyr728 (Fig. 3*B*).

In light of our results, we propose a model in which phosphorylation of Tyr728 may regulate the transition between the scaffolding and the catalytic function of KSR1. Whereas autophosphorylation of Ser722 would activate the kinase activity of KSR1 towards MEK, phosphorylation of Tyr728 by LCK would facilitate the autophosphorylation of Ser722, support the face-to-face binding of MEK to KSR1 for phosphorylation of MEK by KSR1 and counteract the side-to-side heterodimerization of KSR1 with a regulatory RAF molecule preventing the release of MEK activation segment for phosphorylation by catalytic RAF.

In this work we could show that the proliferation of KSR1-deficient MEFs infected with the KSR1-Y728F mutant was significantly increased in comparison to MEFs infected with KSR1 WT (Fig. 5), although the overall MEK and ERK phosphorylation in the lysates was unchanged (data not shown). Since LCK is expressed specifically in lymphocytes, which other tyrosine kinase(s) come(s) into question for phosphorylation of the KSR1-Tyr728 in MEFs? One possible candidate might be c-Src. Indeed, it has been previously shown that e.g. Tyr340/341 in C-RAF and the analogues residues in A-RAF can be phosphorylated by both, c-Src and LCK (32, 53, 54), suggesting that these two kinases share similar substrates. Furthermore, Kilkenny *et al.* (55) reported that MEFs expressing endogenous c-Src exhibit significantly higher FGF- and EGF-induced proliferation rates than cells lacking c-Src, whereas overexpression of c-Src reduced cell proliferation to the level of c-Src knockout MEFs. This indicates that c-Src has positive as well as negative regulatory effects on FGF and EGF signaling. Interestingly, despite the difference in cell proliferation, the level of ERK activation was similar in cells with either endogenous expression or overexpression of c-Src (55). Although the mechanism underlying the negative effects of c-Src overexpression were not addressed in the study by Kilkenny *et al.* (55), our data suggest that phosphorylation of KSR1-Tyr728 by c-Src might

be one possible mechanism. This assumption is supported by the previously published observation that KSR1 specifically blocks growth factor and RAS-induced phosphorylation and activation of Elk-1 (a physiological substrate of ERK involved in regulation of cell proliferation, differentiation and apoptosis), without affecting the overall activation of ERK itself (56). Of note, this effect of KSR1 on Elk-1 appears to require the integrity of its kinase domain, since a kinase-deficient mutant of KSR1 does not inhibit Elk-1, but even enhances both Elk-1 phosphorylation and transactivation activity in unstimulated cells (56). Moreover, KSR1 (the isoform whose function can be regulated by the lymphocyte-specific tyrosine kinase LCK), but not KSR2, is essential for proper activation of the MAPK pathway and biological output in primary T lymphocytes (57). It has been reported that KSR1 modulates the sensitivity of MAPK pathway activation in T cells without altering fundamental system outputs. Accordingly, the level of KSR1 expression is carefully regulated during T cells maturation relative to the components of the MAPK module (57). The results from our proliferation experiments, taken together with the above-described conclusions from other authors, suggest that Tyr728 phosphorylation of KSR1 by LCK is of major physiological relevance and not a simple artifact of transient transfection and/or overexpression. In conclusion, we have identified a novel regulatory phosphorylation site in KSR1 – the Tyr728 – and shown that this tyrosine is phosphorylated by LCK. Furthermore, we propose KSR1 as a control point used to fine-tune cellular responses by regulating the transition between its scaffolding and catalytic functions.

REFERENCES

1. Clapéron, A., and Therrien, M. (2007) KSR and CNK: two scaffolds regulating RAS-mediated RAF activation. *Oncogene* **26**, 3143–58
2. Udell, C. M., Rajakulendran, T., Sicheri, F., and Therrien, M. (2011) Mechanistic principles of RAF kinase signaling. *Cell Mol Life Sci* **68**, 553–65
3. Lozano, J., Xing, R., Cai, Z., Jensen, H. L., Trempus, C., Mark, W., Cannon, R., and Kolesnick, R. (2003) Deficiency of kinase suppressor of Ras1 prevents oncogenic ras signaling in mice. *Cancer Res* **63**, 4232–8
4. Therrien, M., Chang, H. C., Solomon, N. M., Karim, F. D., Wassarman, D. A., and Rubin, G. M. (1995) KSR, a novel protein kinase required for RAS signal transduction. *Cell* **83**, 879–88
5. Channavajhala, P. L., Wu, L., Cuozzo, J. W., Hall, J. P., Liu, W., Lin, L.-L., and Zhang, Y. (2003) Identification of a novel human kinase supporter of Ras (hKSR-2) that functions as a negative regulator of Cot (Tpl2) signaling. *J Biol Chem* **278**, 47089–97
6. Sundaram, M., and Han, M. (1995) The C. elegans ksr-1 gene encodes a novel Raf-related kinase involved in Ras-mediated signal transduction. *Cell* **83**, 889–901
7. Kornfeld, K., Hom, D. B., and Horvitz, H. R. (1995) The ksr-1 gene encodes a novel protein kinase involved in Ras-mediated signaling in C. elegans. *Cell* **83**, 903–13
8. Michaud, N. R., Therrien, M., Cacace, A., Edsall, L. C., Spiegel, S., Rubin, G. M., and Morrison, D. K. (1997) KSR stimulates Raf-1 activity in a kinase-independent manner. *Proc Natl Acad Sci U S A* **94**, 12792–6
9. Denouel-Galy, A., Douville, E. M., Warne, P. H., Papin, C., Laugier, D., Calothy, G., Downward, J., and Eychène, A. (1998) Murine Ksr interacts with MEK and inhibits Ras-induced transformation. *Curr Biol* **8**, 46–55
10. Stewart, S., Sundaram, M., Zhang, Y., Lee, J., Han, M., and Guan, K. L. (1999) Kinase suppressor of Ras forms a multiprotein signaling complex and modulates MEK localization. *Mol Cell Biol* **19**, 5523–34
11. Zhang, Y., Yao, B., Delikat, S., Bayoumy, S., Lin, X. H., Basu, S., McGinley, M., Chan-Hui, P. Y., Lichenstein, H., and Kolesnick, R. (1997) Kinase suppressor of Ras is ceramide-activated protein kinase. *Cell* **89**, 63–72
12. Yan, F., and Polk, D. B. (2001) Kinase suppressor of ras is necessary for tumor necrosis factor alpha activation of extracellular signal-regulated kinase/mitogen-activated protein kinase in intestinal epithelial cells. *Cancer Res* **61**, 963–9

13. Brennan, D. F., Dar, A. C., Hertz, N. T., Chao, W. C. H., Burlingame, A. L., Shokat, K. M., and Barford, D. (2011) A Raf-induced allosteric transition of KSR stimulates phosphorylation of MEK. *Nature* **472**, 366–9
14. Kamps, M. P., and Sefton, B. M. (1986) Neither arginine nor histidine can carry out the function of lysine-295 in the ATP-binding site of p60src. *Mol Cell Biol* **6**, 751–7
15. Roy, F., Laberge, G., Douziech, M., Ferland-McCollough, D., and Therrien, M. (2002) KSR is a scaffold required for activation of the ERK/MAPK module. *Genes Dev* **16**, 427–38
16. Nguyen, A., Burack, W. R., Stock, J. L., Kortum, R., Chaika, O. V, Afkarian, M., Muller, W. J., Murphy, K. M., Morrison, D. K., Lewis, R. E., McNeish, J., and Shaw, A. S. (2002) Kinase suppressor of Ras (KSR) is a scaffold which facilitates mitogen-activated protein kinase activation in vivo. *Mol Cell Biol* **22**, 3035–45
17. Cacace, A. M., Michaud, N. R., Therrien, M., Mathes, K., Copeland, T., Rubin, G. M., and Morrison, D. K. (1999) Identification of constitutive and ras-inducible phosphorylation sites of KSR: implications for 14-3-3 binding, mitogen-activated protein kinase binding, and KSR overexpression. *Mol Cell Biol* **19**, 229–40
18. Therrien, M., Michaud, N. R., Rubin, G. M., and Morrison, D. K. (1996) KSR modulates signal propagation within the MAPK cascade. *Genes Dev* **10**, 2684–95
19. Jacobs, D., Glossip, D., Xing, H., Muslin, A. J., and Kornfeld, K. (1999) Multiple docking sites on substrate proteins form a modular system that mediates recognition by ERK MAP kinase. *Genes Dev* **13**, 163–75
20. Rajakulendran, T., Sahmi, M., Lefrançois, M., Sicheri, F., and Therrien, M. (2009) A dimerization-dependent mechanism drives RAF catalytic activation. *Nature* **461**, 542–5
21. Xing, H., Kornfeld, K., and Muslin, A. J. (1997) The protein kinase KSR interacts with 14-3-3 protein and Raf. *Curr Biol* **7**, 294–300
22. Bell, B., Xing, H., Yan, K., Gautam, N., and Muslin, A. J. (1999) KSR-1 binds to G-protein betagamma subunits and inhibits beta gamma-induced mitogen-activated protein kinase activation. *J Biol Chem* **274**, 7982–6
23. Smith, F. D., Langeberg, L. K., Cellurale, C., Pawson, T., Morrison, D. K., Davis, R. J., and Scott, J. D. (2010) AKAP-Lbc enhances cyclic AMP control of the ERK1/2 cascade. *Nat Cell Biol* **12**, 1242–9
24. Müller, J., Ory, S., Copeland, T., Piwnica-Worms, H., and Morrison, D. K. (2001) C-TAK1 regulates Ras signaling by phosphorylating the MAPK scaffold, KSR1. *Mol Cell* **8**, 983–93
25. Ory, S., Zhou, M., Conrads, T. P., Veenstra, T. D., and Morrison, D. K. (2003) Protein phosphatase 2A positively regulates Ras signaling by dephosphorylating KSR1 and Raf-1 on critical 14-3-3 binding sites. *Curr Biol* **13**, 1356–64
26. McKay, M. M., Ritt, D. A., and Morrison, D. K. (2009) Signaling dynamics of the KSR1 scaffold complex. *Proc Natl Acad Sci U S A* **106**, 11022–7
27. McKay, M. M., and Morrison, D. K. (2007) Caspase-dependent cleavage disrupts the ERK cascade scaffolding function of KSR1. *J Biol Chem* **282**, 26225–34
28. Qiao, Y., Molina, H., Pandey, A., Zhang, J., and Cole, P. A. (2006) Chemical rescue of a mutant enzyme in living cells. *Science* **311**, 1293–7
29. Biscardi, J. S., Maa, M. C., Tice, D. A., Cox, M. E., Leu, T. H., and Parsons, S. J. (1999) c-Src-mediated phosphorylation of the epidermal growth factor receptor on Tyr845 and Tyr1101 is associated with modulation of receptor function. *J Biol Chem* **274**, 8335–43
30. Amrein, K. E., Panholzer, B., Molnos, J., Flint, N. A., Scheffler, J., Lahm, H. W., Bannwarth, W., and Burn, P. (1994) Mapping of the p56lck-mediated phosphorylation of GAP and analysis of its influence on p21ras-GTPase activity in vitro. *Biochim Biophys Acta* **1222**, 441–6
31. Park, S., Liu, X., Pawson, T., and Jove, R. (1992) Activated Src tyrosine kinase phosphorylates Tyr-457 of bovine GTPase-activating protein (GAP) in vitro and the corresponding residue of rat GAP in vivo. *J Biol Chem* **267**, 17194–200
32. Fabian, J. R., Daar, I. O., and Morrison, D. K. (1993) Critical tyrosine residues regulate the enzymatic and biological activity of Raf-1 kinase. *Mol Cell Biol* **13**, 7170–9

33. Marais, R., Light, Y., Paterson, H. F., Mason, C. S., and Marshall, C. J. (1997) Differential regulation of Raf-1, A-Raf, and B-Raf by oncogenic ras and tyrosine kinases. *J Biol Chem* **272**, 4378–83
34. Diaz, B., Barnard, D., Filson, A., MacDonald, S., King, A., and Marshall, M. (1997) Phosphorylation of Raf-1 serine 338-serine 339 is an essential regulatory event for Ras-dependent activation and biological signaling. *Mol Cell Biol* **17**, 4509–16
35. Klinghoffer, R. A., Sachsenmaier, C., Cooper, J. A., and Soriano, P. (1999) Src family kinases are required for integrin but not PDGFR signal transduction. *EMBO J* **18**, 2459–71
36. Winkler, C., Denker, K., Wortelkamp, S., and Sickmann, A. (2007) Silver- and Coomassie-staining protocols: detection limits and compatibility with ESI MS. *Electrophoresis* **28**, 2095–9
37. Burkhart, J. M., Schumbrutzki, C., Wortelkamp, S., Sickmann, A., and Zahedi, R. P. (2012) Systematic and quantitative comparison of digest efficiency and specificity reveals the impact of trypsin quality on MS-based proteomics. *J Proteomics* **75**, 1454–62
38. Beck, F., Lewandrowski, U., Wiltfang, M., Feldmann, I., Geiger, J., Sickmann, A., and Zahedi, R. P. (2011) The good, the bad, the ugly: validating the mass spectrometric analysis of modified peptides. *Proteomics* **11**, 1099–109
39. Burkhart, J. M., Premsler, T., and Sickmann, A. (2011) Quality control of nano-LC-MS systems using stable isotope-coded peptides. *Proteomics* **11**, 1049–57
40. Olsen, J. V, De Godoy, L. M. F., Li, G., Macek, B., Mortensen, P., Pesch, R., Makarov, A., Lange, O., Horning, S., and Mann, M. (2005) Parts per million mass accuracy on an Orbitrap mass spectrometer via lock mass injection into a C-trap. *Mol Cell Proteomics* **4**, 2010–21
41. Kessner, D., Chambers, M., Burke, R., Agus, D., and Mallick, P. (2008) ProteoWizard: open source software for rapid proteomics tools development. *Bioinformatics* **24**, 2534–6
42. Vaudel, M., Barsnes, H., Berven, F. S., Sickmann, A., and Martens, L. (2011) SearchGUI: An open-source graphical user interface for simultaneous OMSSA and X!Tandem searches. *Proteomics* **11**, 996–9
43. Vaudel, M., Breiter, D., Beck, F., Rahnenführer, J., Martens, L., and Zahedi, R. P. (2013) D-score: A search engine independent MD-score. *Proteomics* **13**, 1036–41
44. Xia, F., Li, J., Hickey, G. W., Tsurumi, A., Larson, K., Guo, D., Yan, S.-J., Silver-Morse, L., and Li, W. X. (2008) Raf activation is regulated by tyrosine 510 phosphorylation in Drosophila. *PLoS Biol* **6**, e128
45. Kortum, R. L., and Lewis, R. E. (2004) The molecular scaffold KSR1 regulates the proliferative and oncogenic potential of cells. *Mol Cell Biol* **24**, 4407–16
46. Dougherty, D. A. (2007) Cation-{pi} Interactions Involving Aromatic Amino Acids. *J. Nutr.* **137**, 1504S–1508
47. Jiménez, J. L., Hegemann, B., Hutchins, J. R. A., Peters, J.-M., and Durbin, R. (2007) A systematic comparative and structural analysis of protein phosphorylation sites based on the mtcPTM database. *Genome Biol* **8**, R90
48. Hanks, S. K., and Hunter, T. (1995) Protein kinases 6. The eukaryotic protein kinase superfamily: kinase (catalytic) domain structure and classification. *FASEB J* **9**, 576–96
49. Goettel, J. A., Liang, D., Hilliard, V. C., Edelblum, K. L., Broadus, M. R., Gould, K. L., Hanks, S. K., and Polk, D. B. (2011) KSR1 is a functional protein kinase capable of serine autophosphorylation and direct phosphorylation of MEK1. *Exp Cell Res* **317**, 452–63
50. Abe, M. K., Kahle, K. T., Saelzler, M. P., Orth, K., Dixon, J. E., and Rosner, M. R. (2001) ERK7 is an autoactivated member of the MAPK family. *J Biol Chem* **276**, 21272–9
51. Cole, A., Frame, S., and Cohen, P. (2004) Further evidence that the tyrosine phosphorylation of glycogen synthase kinase-3 (GSK3) in mammalian cells is an autophosphorylation event. *Biochem J* **377**, 249–55
52. Lochhead, P. A., Sibbet, G., Morrice, N., and Cleghon, V. (2005) Activation-loop autophosphorylation is mediated by a novel transitional intermediate form of DYRKs. *Cell* **121**, 925–36

53. Marais, R., Light, Y., Paterson, H. F., Mason, C. S., and Marshall, C. J. (1997) Differential regulation of Raf-1, A-Raf, and B-Raf by oncogenic ras and tyrosine kinases. *J Biol Chem* **272**, 4378–83
54. Baljuls, A., Mueller, T., Drexler, H. C. A., Hekman, M., and Rapp, U. R. (2007) Unique N-region determines low basal activity and limited inducibility of A-RAF kinase: the role of N-region in the evolutionary divergence of RAF kinase function in vertebrates. *J Biol Chem* **282**, 26575–90
55. Kilkenny, D. M., Rocheleau, J. V, Price, J., Reich, M. B., and Miller, G. G. (2003) c-Src regulation of fibroblast growth factor-induced proliferation in murine embryonic fibroblasts. *J Biol Chem* **278**, 17448–54
56. Sugimoto, T., Stewart, S., Han, M., and Guan, K. L. (1998) The kinase suppressor of Ras (KSR) modulates growth factor and Ras signaling by uncoupling Elk-1 phosphorylation from MAP kinase activation. *EMBO J* **17**, 1717–27
57. Lin, J., Harding, A., Giurisato, E., and Shaw, A. S. (2009) KSR1 modulates the sensitivity of mitogen-activated protein kinase pathway activation in T cells without altering fundamental system outputs. *Mol Cell Biol* **29**, 2082–91
58. Cabeza-Arvelaiz, Y., and Schiestl, R. H. (2012) Transcriptome analysis of a rotenone model of parkinsonism reveals complex I-tied and -untied toxicity mechanisms common to neurodegenerative diseases. *PloS One* **7**, e44700

Acknowledgements—We thank Robert E. Lewis (University of Nebraska Medical Center, Omaha) for generously providing the immortalized KSR1$^{-/-}$ MEFs and the bicistronic FLAG-tagged murine KSR1 wild type construct as well as empty MSCV-IRES-GFP and ecotropic packaging vector; Ann-Cathrin Winkler and Christine Siegl (Department of Microbiology, University of Wuerzburg) for help with FACS analysis; Walter Kolch (Systems Biology Ireland) and Mirko Hekman for critical reading of the manuscript.

FOOTNOTES

*****This work was supported by Deutsche Forschungsgemeinschaft (DFG) Grant SFB 487 (projects C3 to U.R.R. and B2 to T.M.), by University of Wuerzburg, Fellowship „Chancengleichheit für Frauen in Forschung und Lehre“ to C.S., by a DFG Fellowship to A.B., and by the Science Foundation Ireland (SFI) under grant 06/CE/B1129. L.K. and R.Z. thank the “Ministerium für Innovation, Wissenschaft und Forschung des Landes Nordrhein-Westfalen” for continuous support.

[1]To whom correspondence may be addressed: Department of Microbiology, Biocenter, University of Wuerzburg, Am Hubland, 97074 Wuerzburg, Germany. Tel.: 49-931-31-84401; Fax: 49-931-31-84402; E-mail: thomas.rudel@biozentrum.uni-wuerzburg.de.

[2]To whom correspondence may be addressed: Systems Biology Ireland, Conway Institute, University College Dublin, Belfield, Dublin 4, Ireland. Tel.: 353-1-7166979; E-mail: angela.baljuls@ucd.ie.

[3]The abbreviations used are: CR, conserved region; MEFs, mouse embryonic fibroblasts; MS, mass spectrometry; LC, liquid chromatography; CID, collision-induced dissociation; MSA, multistage activation; VMD, visual molecular dynamics; MD, molecular dynamics; r.m.s., root mean square; PDB, protein data bank; WT, wild type; KD, kinase domain; IB, immunoblot; PD, pull-down; SD, standard deviation.

FIGURE LEGENDS

FIGURE 1. **LCK binds to KSR1 and phosphorylates it on tyrosine residue(s).** *A*, kinase-active (Y505F) and kinase-inactive (K273E/Y505F) LCK were coexpressed with GST-KSR1 in COS7 cells. Phosphorylation levels of precipitated GST-KSR1 and KSR1-bound LCK were detected by use of an anti-phospho-tyrosine antibody. *B*, COS7 cells were transfected with LCK-Y505F and GST-KSR1 and

treated with LCK inhibitor III (100μM) or solvent (DMSO) 2h prior to cell harvesting. GST-KSR1 was precipitated and tested for binding of LCK and tyrosine phosphorylation. *PD*, pull-down; *IB*, immunoblot; α, anti.

FIGURE 2. **LCK phosphorylates KSR1 on Tyr728.** *A*, amino acids sequence of the murine KSR1 depicting phosphorylation sites identified by MS analysis. The known phosphorylation sites are highlighted in green, whereas the newly identified confident phosphorylation sites are highlighted in red. The conserved regulatory domains are grey-shaded. *B* and *C*, GST-tagged KSR1 WT and mutants Y673F and Y728F were coexpressed with active LCK in COS7 cells and precipitated by use of glutathione-sepharose beads. The levels of tyrosine phosphorylation were detected by an anti-phospho-tyrosine antibody.

FIGURE 3. **Tyr673 is crucial for maintaining the structure of the KSR1 kinase domain.** *A*, schematic presentation of KSR1 and multiple sequence alignment of KSR1 from different species. *B*, pairwise alignment of murine KSR1 and KSR2. The amino acid sequences were obtained from NCBI (accession numbers: NP_038599, Q8IVT5, NP_001101754, NP_001186688, XP_684771, AAF52021, NP_509396, NP_001108017) and merged with Jalview software. *C-F*, GST-tagged KSR1 WT or KSR1-Y673F mutant were transfected into COS7 cells. The cells were lysed and subjected to GST-precipitation by use of glutathione-sepharose beads. Amount and phosphorylation levels of (co)precipitated proteins were determined by use of appropriate antibodies. For diagrams, data from three independent experiments were quantified by optical densitometry. Bar diagrams show the relative amount of phosphorylated MEK bound to KSR1, where 1-fold represents phosphorylation level of MEK interacting with KSR1 WT (*D*) or the relative amount of B-RAF bound to KSR1, where 1-fold represents B-RAF interacting with KSR1 WT (*F*). Data are presented as mean ± SD of the respective measured parameters. P values: ns (not significant), ≥ 0.05; ***** (significant), $P < 0.05$; ****** (highly significant), $P < 0.01$; ******* (extremely significant), $P < 0.001$ versus corresponding WT control.

FIGURE 4. **Tyr728 regulates activation of MEK.** GST-tagged KSR1 WT and KSR1-Y728F were transfected into COS7 cells and precipitated with glutathione-sepharose beads. Amount and phosphorylation levels of (co)precipitated proteins were determined by use of appropriate antibodies. Quantifications were done as described in Fig. 3.

FIGURE 5. **Substitution of Tyr728 in KSR1 promotes proliferation of MEFs.** $KSR1^{-/-}$ MEFs were infected with retroviruses carrying empty vector, KSR1 WT or KSR1-Y728F. Infected MEFs were sorted by FACS according to the levels of GFP fluorescence. Four fractions of infected MEFs were collected and KSR1 expression was tested by immunoblotting (*A*). For proliferation assay, fraction number four was used. Proliferation of infected MEFs was analyzed by counting living cells using FACS on day 3, 6, 9, and 12 after synchronization of cell cycle. During the timeframe of the assay MEFs were kept in the exponential growth phase by trypsinizing and seeding every third day. The cell counts were used to calculate the population doubling time (PDT) (*B*) and determine the cell proliferation curves (*C*) as described in (58). *Points*, mean of at least three independent experiments; *bars*, SD. P values: ns (not significant), ≥ 0.05; ***** (significant), $P < 0.05$; ****** (highly significant), $P < 0.01$; ******* (extremely significant), $P < 0.001$ versus corresponding empty vector control.

FIGURE 6. **Structure of the mKSR1/MEK1 kinase domain complex with focus on phospho-Tyr728.** *A*, overall view of the mKSR1 kinase domain (KD) modeled by use of the structure of hKSR2(KD) as a template (13). *B*, detailed view of direct hydrogen bonds formed between the phosphate group of phospho-Tyr728 and the surrounding residues in mKSR1(KD). *C*, overall view of the mKSR1/MEK1 complex modeled by docking the structure of mKSR1(KD) from *A* onto the template complex KSR2/MEK1 (13). *D*, close-up view of the interacting surface in mKSR1(KD) and MEK1(KD).

FIGURE 7. **Substitution of Arg649 and Tyr728 with different amino acids results in distinct outcomes for MEK binding and phosphorylation.** *A* and *B*, GST-KSR1 WT and indicated mutants

were expressed in COS7 cells and precipitated by use of glutathione-sepharose beads. Amount and phosphorylation levels of (co)precipitated proteins were determined by use of appropriate antibodies. *C*, data from three independent experiments were quantified by optical densitometry. Bar diagram shows the relative amount of phosphorylated MEK bound to KSR1, where 1-fold represents phosphorylation level of MEK interacting with KSR1 WT. Data are presented as mean ± SD of the respective measured parameters. P values: ns (not significant), ≥ 0.05; ***** (significant), $P < 0.05$; ****** (highly significant), $P < 0.01$; ******* (extremely significant), $P < 0.001$ versus corresponding WT control.

FIGURE 8. **Fluctuations of backbone coordinate in Tyr728-phosphorylated and Tyr728-non-phosphorylated KSR1 analyzed by MD simulations.** *A*, the model of the mKSR1(KD) (stereo view). The structural elements analyzed by MD simulation are highlighted in different colors. Red, the helical element harboring Tyr728; dark blue, the activation loop; green, the short helix comprising residues 643 to 649; magenta, the catalytic loop (residues 679 to 686); cyan, the αG helix (which is part of the KSR1 interface to MEK1); yellow, the potential interface to RAF kinases. The phospho-Tyr728 and ATP moieties are shown as sticks; the magnesium ion is indicated as green sphere. The loop regions are highlighted with the Cα atoms shown as small spheres. *B–G*, r.m.s. deviation for backbone atoms of indicated structural elements during the 5ns trajectory molecular dynamics simulation using the software NAMD (NAMD, Scalable Molecular Dynamics software package). The curve representing backbone atom fluctuations of Tyr728-non-phosphorylated KSR1(KD) is shown in black; the red curve represents the same of Tyr728-phosphorylated KSR1(KD).

FIGURE 9. **MD simulations suggest that phosphorylation of Tyr728 may alter KSR1 kinase activity or/and its interaction with MEK.** *A*, close-up view of the polar interactions between the phosphate group of phospho-Tyr728 and the conserved Lys685 in the catalytic loop of KSR1(KD). The ATP and magnesium ion are presented as ball-and-stick models (also in *C*); the Asp683, which is also involved in the phosphate transfer is shown as sticks. *B*, the variation in distance between the amino nitrogen atom of Lys685 and the γ-phosphate atom of the ATP molecule is shown for Tyr728-phosphorylated (red curve) and Tyr728-non-phosphorylated KSR1(KD) (black curve). During the trajectory of the MD simulation the amino group of the conserved Lys685 in the catalytic loop of KSR1(KD) becomes conformationally fixed between the phosphate group of phospho-Tyr728 and the γ-phosphate group of the ATP molecule, such that it can ideally facilitate phosphate transfer from the ATP to an acceptor hydroxyl group in a substrate (see red curve). In case of Tyr728 being not phosphorylated the distance between the amino group of Lys685 and the γ-phosphate of the ATP molecule varies throughout the MD simulation indicating that the groups involved in the catalytic cycle of phosphate transfer are not properly lined up over time (black curve). *C*, close-up view of the potential long-range interaction between phospho-Tyr728 and the αG helix of KSR1, which is the major contact surface in the KSR1(KD)/MEK1 interaction. To analyze possible conformation rearrangements in the αG helix, the variation in distance between the Cα-atom of Tyr728 and Ala778 was monitored throughout the 5ns trajectory of the molecular dynamics simulation (*D*). The comparison of the distance variation between Tyr728-phosphorylated (red curve) and Tyr728-non-phosphorylated KSR1(KD) (black curve) indicated that with Tyr728 being phosphorylated the distance between Tyr728 and the αG helix of the KSR1(KD) is smaller and a more compact interface might facilitate MEK1 binding.

Figure 1

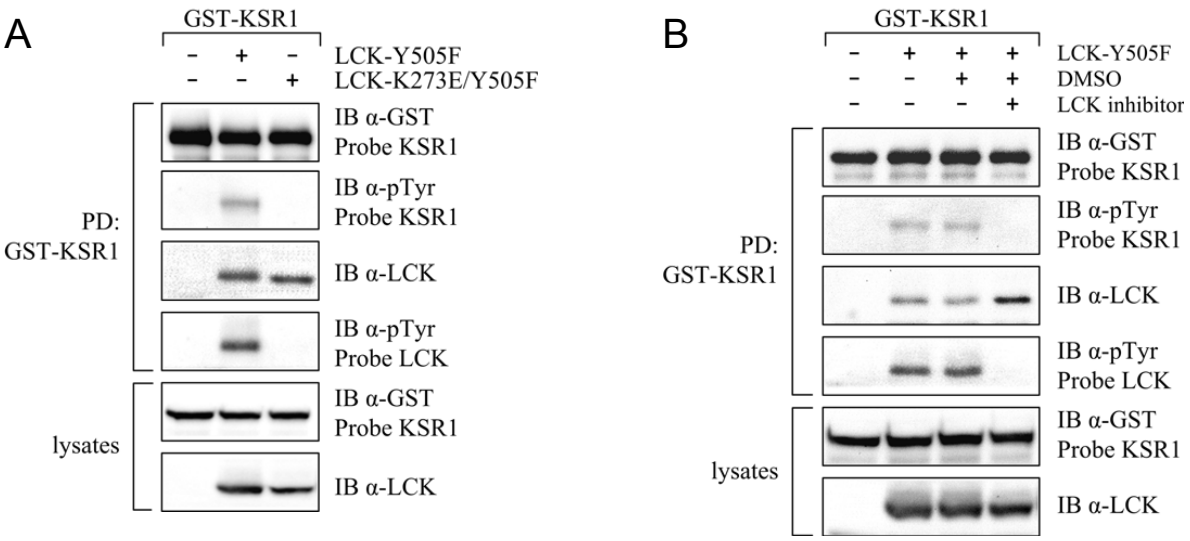
A
GST-KSR1
LCK-Y505F
LCK-K273E/Y505F
IB α-GST
Probe KSR1
IB α-pTyr
Probe KSR1
IB α-LCK
IB α-pTyr
Probe LCK
PD:
GST-KSR1
IB α-GST
Probe KSR1
IB α-LCK
lysates
B
GST-KSR1
LCK-Y505F
DMSO
LCK inhibitor
IB α-GST
Probe KSR1
IB α-pTyr
Probe KSR1
IB α-LCK
IB α-pTyr
Probe LCK
PD:
GST-KSR1
IB α-GST
Probe KSR1
IB α-LCK
lysates

Figure 2

A


Ser33
CA1
Thr58
Ser63
Thr98
Ser103
Ser183
Ser190
Ser224
Ser234
Ser253 Thr256
Thr259/Thr260
Thr274
CA2
Ser295/Ser297/Ser300
Thr310
Ser320
CA3
Thr390
Ser392/Ser395
Thr411
CA4
Ser439
Ser443/Ser450
Ser454
Thr457/Thr458/Ser463
Ser472
Thr500
Ser518
Ser547
CA5
Ser722
Tyr728
Ser838
Thr865

B

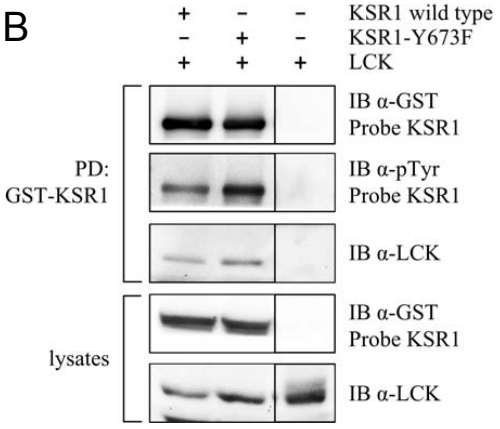
+ − − KSR1 wild type
− + − KSR1-Y673F
+ + + LCK
PD: GST-KSR1
IB α-GST Probe KSR1
IB α-pTyr Probe KSR1
IB α-LCK
lysates
IB α-GST Probe KSR1
IB α-LCK

C

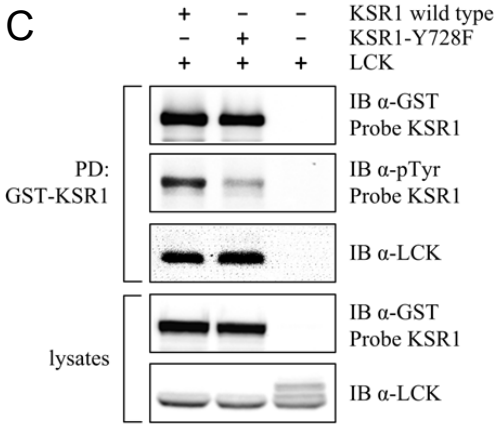
+ − − KSR1 wild type
− + − KSR1-Y728F
+ + + LCK
PD: GST-KSR1
IB α-GST Probe KSR1
IB α-pTyr Probe KSR1
IB α-LCK
lysates
IB α-GST Probe KSR1
IB α-LCK

Figure 3

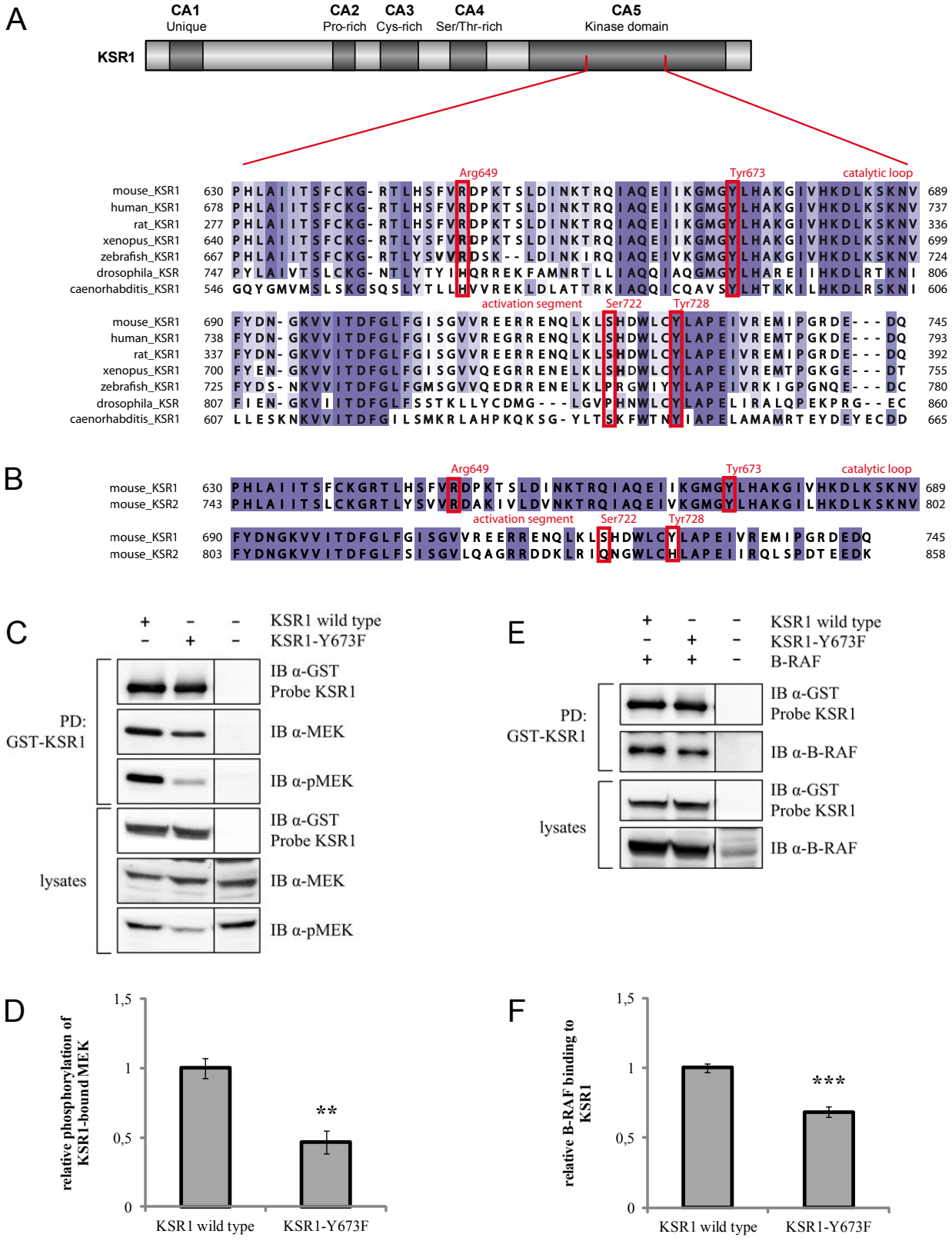
A
CA1
Unique
CA2
Pro-rich
CA3
Cys-rich
CA4
Ser/Thr-rich
CA5
Kinase domain
KSR1
Arg649
Tyr673
catalytic loop
activation segment
Ser722
Tyr728
mouse_KSR1
human_KSR1
rat_KSR1
xenopus_KSR1
zebrafish_KSR1
drosophila_KSR
caenorhabditis_KSR1
mouse_KSR2
B
C
KSR1 wild type
KSR1-Y673F
PD:
GST-KSR1
IB α-GST
Probe KSR1
IB α-MEK
IB α-pMEK
lysates
E
B-RAF
IB α-B-RAF
D
relative phosphorylation of KSR1-bound MEK
1,5
1
0,5
0
**
KSR1 wild type
KSR1-Y673F
F
relative B-RAF binding to KSR1
***

Figure 4

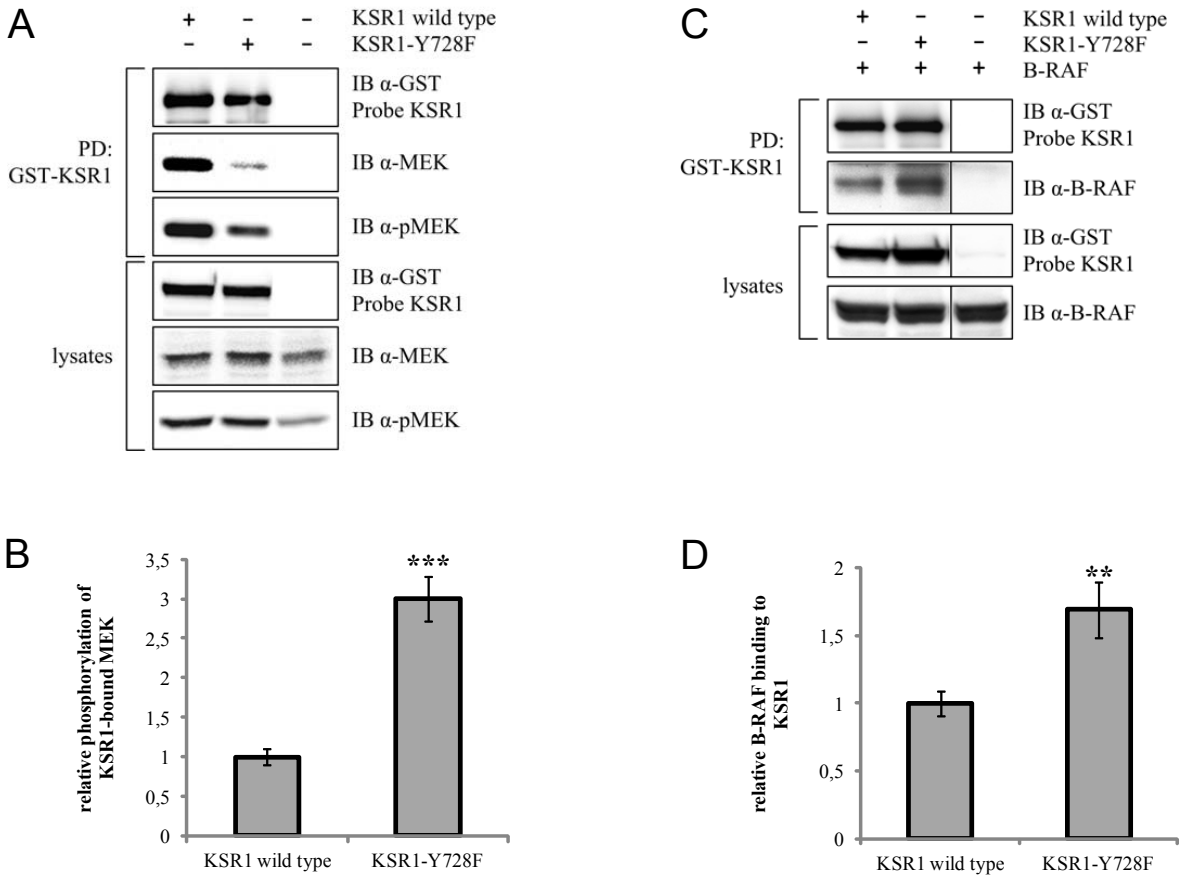
A
+ − − KSR1 wild type
− + − KSR1-Y728F
PD: GST-KSR1
IB α-GST Probe KSR1
IB α-MEK
IB α-pMEK
lysates
IB α-GST Probe KSR1
IB α-MEK
IB α-pMEK
C
+ − − KSR1 wild type
− + − KSR1-Y728F
+ + + B-RAF
PD: GST-KSR1
IB α-GST Probe KSR1
IB α-B-RAF
lysates
IB α-GST Probe KSR1
IB α-B-RAF
B
relative phosphorylation of KSR1-bound MEK
3,5
3
2,5
2
1,5
1
0,5
0
***
KSR1 wild type
KSR1-Y728F
D
relative B-RAF binding to KSR1
2
1,5
1
0,5
0
**
KSR1 wild type
KSR1-Y728F

Figure 5

A

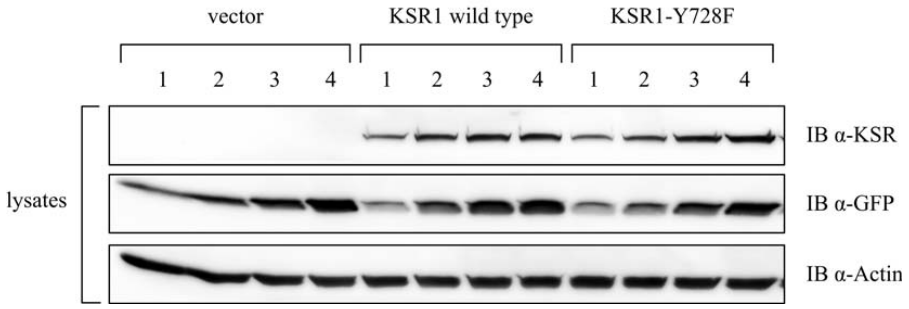
vector
KSR1 wild type
KSR1-Y728F
1 2 3 4 1 2 3 4 1 2 3 4
lysates
IB α-KSR
IB α-GFP
IB α-Actin

B

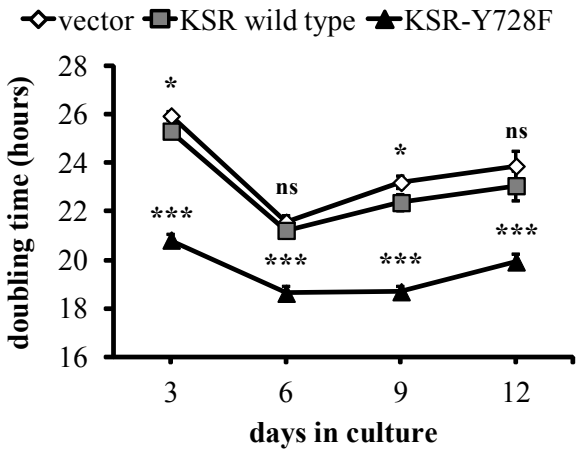
vector
KSR wild type
KSR-Y728F
doubling time (hours)
28
26
24
22
20
18
16
*
ns
*
ns
***
***
***
***
3
6
9
12
days in culture

C

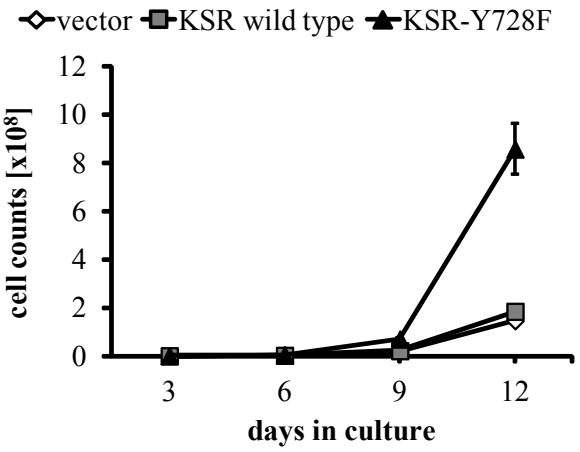
vector
KSR wild type
KSR-Y728F
cell counts [x10⁸]
12
10
8
6
4
2
0
3
6
9
12
days in culture

Figure 6

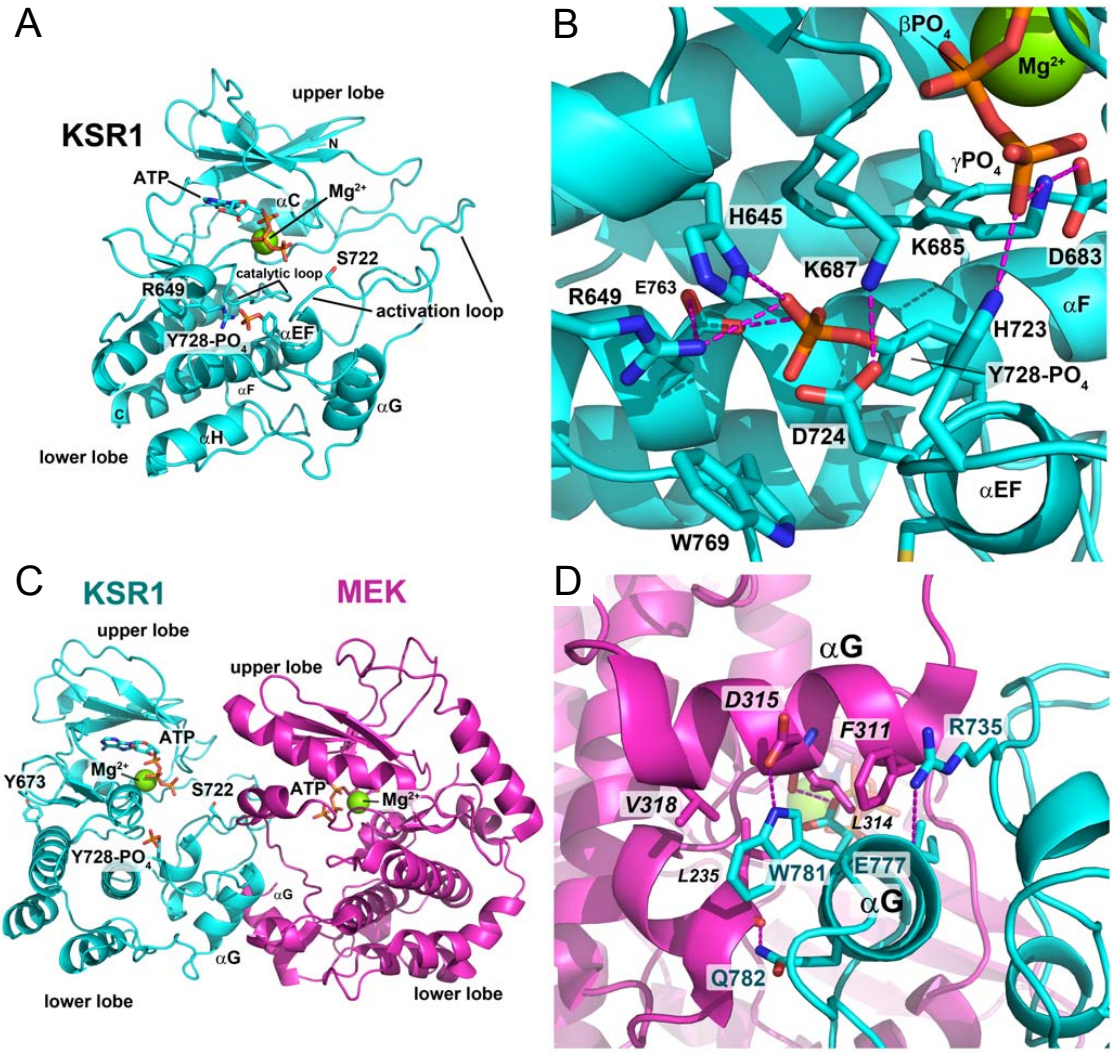
A
KSR1
upper lobe
N
ATP
αC
Mg2+
S722
catalytic loop
R649
activation loop
Y728-PO4
αEF
αF
C
αG
αH
lower lobe
B
βPO4
Mg2+
γPO4
H645
K685
D683
K687
E763
R649
αF
H723
Y728-PO4
D724
αEF
W769
C
KSR1
MEK
upper lobe
upper lobe
ATP
Mg2+
Y673
S722
ATP
Mg2+
Y728-PO4
αG
αG
lower lobe
lower lobe
D
αG
D315
F311
R735
V318
L314
L235
W781
E777
αG
Q782

Figure 7

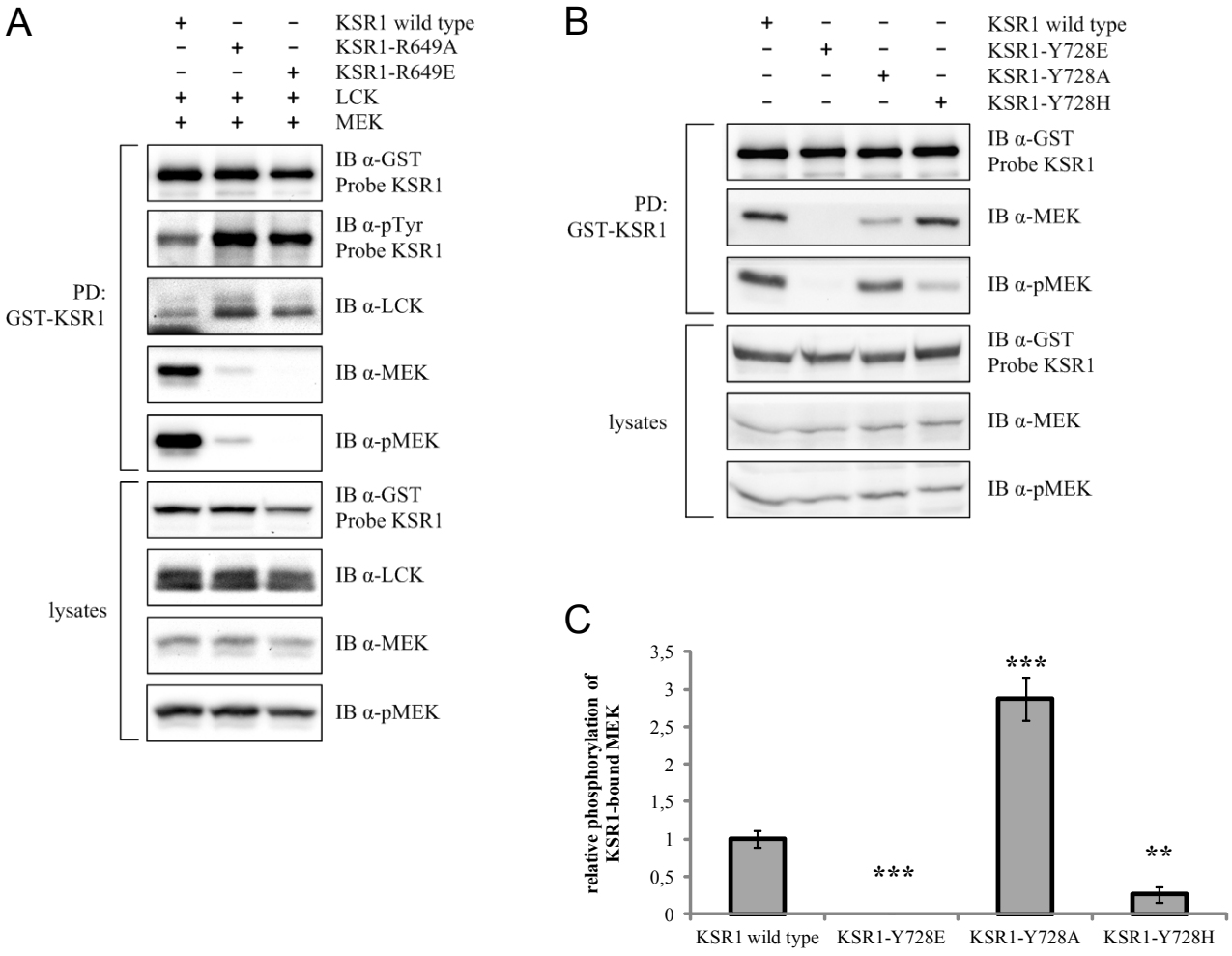
A
+ − − KSR1 wild type
− + − KSR1-R649A
− − + KSR1-R649E
+ + + LCK
+ + + MEK
PD: GST-KSR1
IB α-GST Probe KSR1
IB α-pTyr Probe KSR1
IB α-LCK
IB α-MEK
IB α-pMEK
lysates
IB α-GST Probe KSR1
IB α-LCK
IB α-MEK
IB α-pMEK
B
+ − − − KSR1 wild type
− + − − KSR1-Y728E
− − + − KSR1-Y728A
− − − + KSR1-Y728H
PD: GST-KSR1
IB α-GST Probe KSR1
IB α-MEK
IB α-pMEK
lysates
IB α-GST Probe KSR1
IB α-MEK
IB α-pMEK
C
relative phosphorylation of KSR1-bound MEK
3,5
3
2,5
2
1,5
1
0,5
0
***
***
**
KSR1 wild type
KSR1-Y728E
KSR1-Y728A
KSR1-Y728H

Figure 8

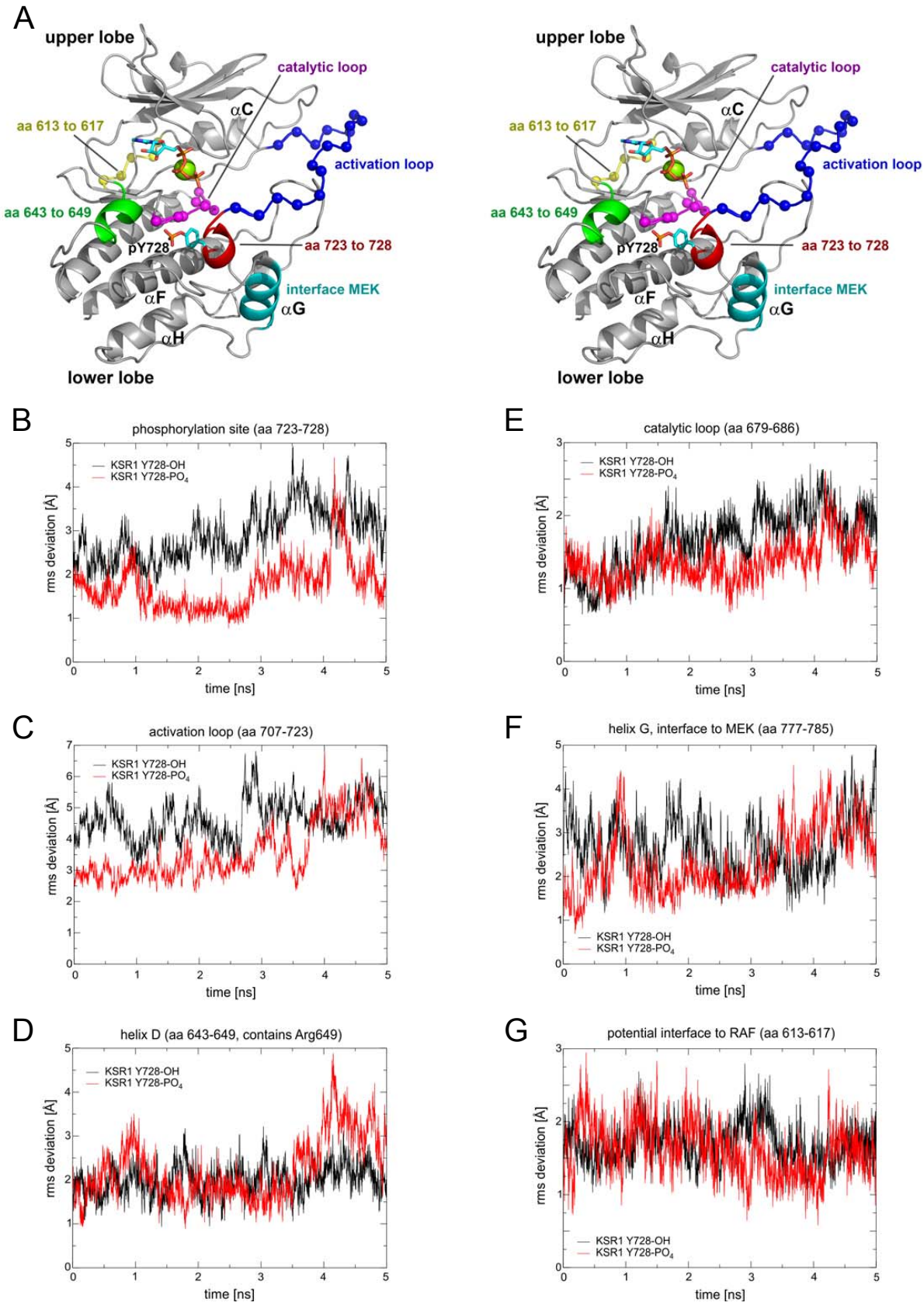
A
upper lobe
catalytic loop
αC
aa 613 to 617
activation loop
aa 643 to 649
pY728
aa 723 to 728
interface MEK
αF
αG
αH
lower loop
B
phosphorylation site (aa 723-728)
C
activation loop (aa 707-723)
D
helix D (aa 643-649, contains Arg649)
E
catalytic loop (aa 679-686)
F
helix G, interface to MEK (aa 777-785)
G
potential interface to RAF (aa 613-617)
KSR1 Y728-OH
KSR1 Y728-PO4
rms deviation [Å]
time [ns]

Figure 9

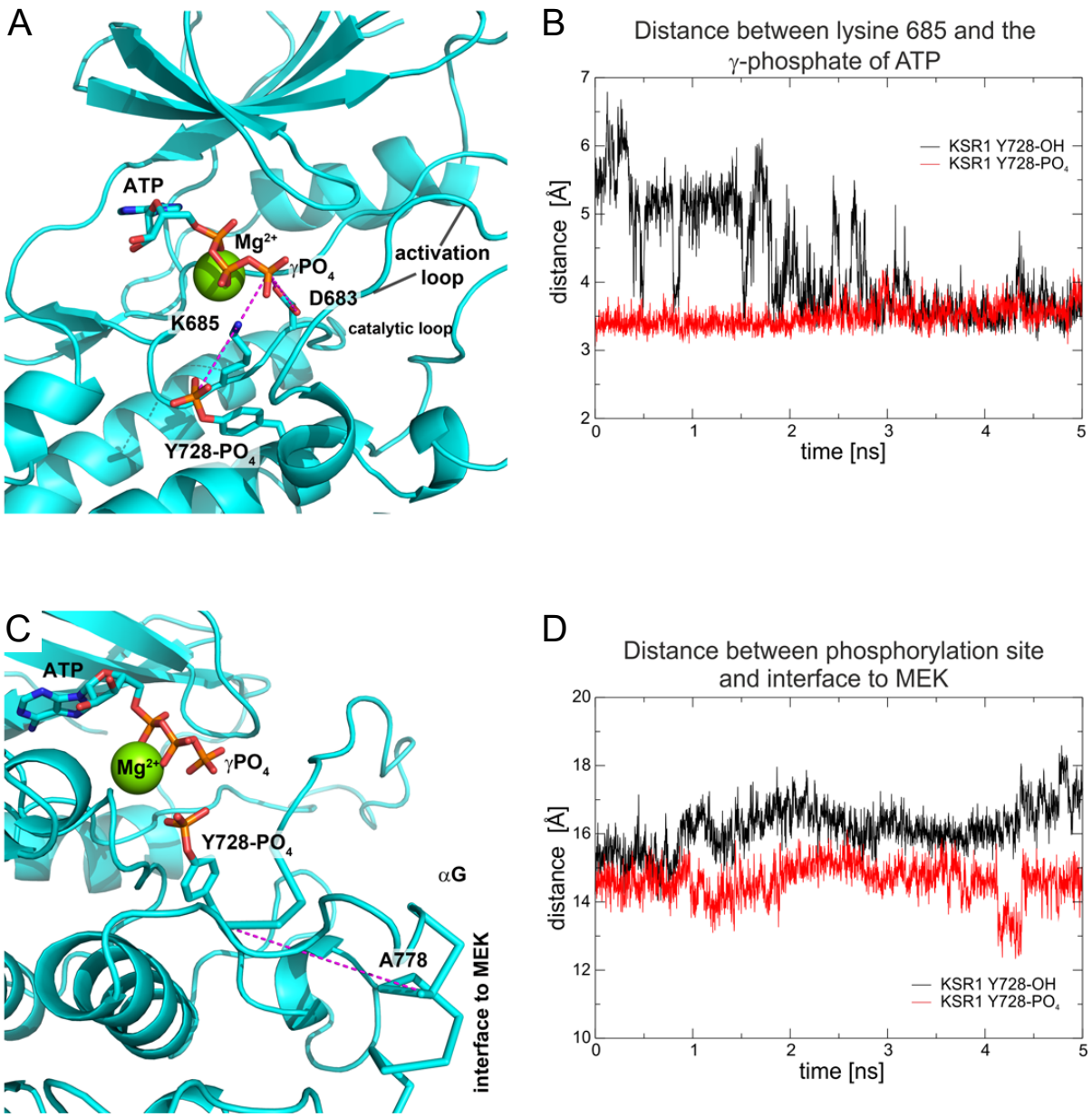
A
ATP
Mg2+
γPO4
activation loop
D683
K685
catalytic loop
Y728-PO4
B
Distance between lysine 685 and the γ-phosphate of ATP
KSR1 Y728-OH
KSR1 Y728-PO4
distance [Å]
time [ns]
C
ATP
Mg2+
γPO4
Y728-PO4
αG
A778
interface to MEK
D
Distance between phosphorylation site and interface to MEK
KSR1 Y728-OH
KSR1 Y728-PO4
distance [Å]
time [ns]